Radiocarbon age-offsets in an arctic lake reveal the long-term response of permafrost carbon to climate change

Benjamin V. Gaglioti[1,2], Daniel H. Mann[3], Benjamin M. Jones[2], John W. Pohlman[4], Michael L. Kunz[3], and Matthew J. Wooller[1,5]

[1]Water and Environmental Research Center, University of Alaska Fairbanks, Fairbanks, Alaska, USA, [2]Alaska Science Center, U.S. Geological Survey, Anchorage, Alaska, USA, [3]Geography Program, School of Natural Resources and Agricultural Science, University of Alaska Fairbanks, Fairbanks, Alaska, USA, [4]Woods Hole Coastal and Marine Science Center, US Geological Survey, Woods Hole, Massachusetts, USA, [5]School of Fisheries and Ocean Sciences, University of Alaska Fairbanks, Fairbanks, Alaska, USA

Abstract Continued warming of the Arctic may cause permafrost to thaw and speed the decomposition of large stores of soil organic carbon (OC), thereby accentuating global warming. However, it is unclear if recent warming has raised the current rates of permafrost OC release to anomalous levels or to what extent soil carbon release is sensitive to climate forcing. Here we use a time series of radiocarbon age-offsets (^{14}C) between the bulk lake sediment and plant macrofossils deposited in an arctic lake as an archive for soil and permafrost OC release over the last 14,500 years. The lake traps and archives OC imported from the watershed and allows us to test whether prior warming events stimulated old carbon release and heightened age-offsets. Today, the age-offset (2 ka; thousand of calibrated years before A.D. 1950) and the depositional rate of ancient OC from the watershed into the lake are relatively low and similar to those during the Younger Dryas cold interval (occurring 12.9–11.7 ka). In contrast, age-offsets were higher (3.0–5.0 ka) when summer air temperatures were warmer than present during the Holocene Thermal Maximum (11.7–9.0 ka) and Bølling-Allerød periods (14.5–12.9 ka). During these warm times, permafrost thaw contributed to ancient OC depositional rates that were ~10 times greater than today. Although permafrost OC was vulnerable to climate warming in the past, we suggest surface soil organic horizons and peat are presently limiting summer thaw and carbon release. As a result, the temperature threshold to trigger widespread permafrost OC release is higher than during previous warming events.

1. Introduction

Thawing of permafrost caused by ongoing warming could perturb the high-latitude carbon cycle and affect global climate [*McGuire et al.*, 2009]. Approximately half of Earth's soil organic carbon (SOC) either resides within or lies above permafrost (perennially frozen ground) [*Tarnocai et al.*, 2009]. Permafrost-associated OC originated as terrestrial-, aquatic-, and marine-derived organic matter incorporated in near-surface sediments over the course of the last several glacial-interglacial cycles [*French*, 2010]. This OC can persist for long periods because permafrost soils are cold, typically nutrient poor, and frequently anoxic, factors that limit decomposition [*McGuire et al.*, 2009; *Schuur et al.*, 2009]. Warming at high latitudes is expected to trigger widespread permafrost thaw, which will increase the exposure of permafrost OC to decomposition, increase the emission of CO_2 and CH_4 to the atmosphere, and thereby contribute to further climate warming [*Walter et al.*, 2006; *Schuur et al.*, 2008; *McGuire et al.*, 2009].

A projected symptom of a warming Arctic is landscape instability caused by thermokarst processes (ground subsidence from permafrost thaw), which exposes subsurface sediment and ancient organic matter to erosion and leaching [*Frey and McClelland*, 2009]. Thermokarst reworks ancient OC to streams, lakes, and marine systems where it is respired [*Kling et al.*, 1991], incorporated into organisms [*Schell*, 1983; *Wooller et al.*, 2012; *Hågvar and Ohlson*, 2013], and/or restored in depositional environments [*Guo et al.*, 2007; *Schreiner et al.*, 2014]. An extreme example of ancient terrestrial subsidies supporting aquatic food webs comes from a 1.3 ka ^{14}C age (thousands of calibrated years before A.D. 1950) of a living long-tailed duck in Arctic Alaska [*Schell*, 1983]. Minerogenic sediment from thermokarst imported to lake systems also impacts water clarity, sediment chemistry, and the composition of primary producers [*Mesquita et al.*, 2010]. The last time
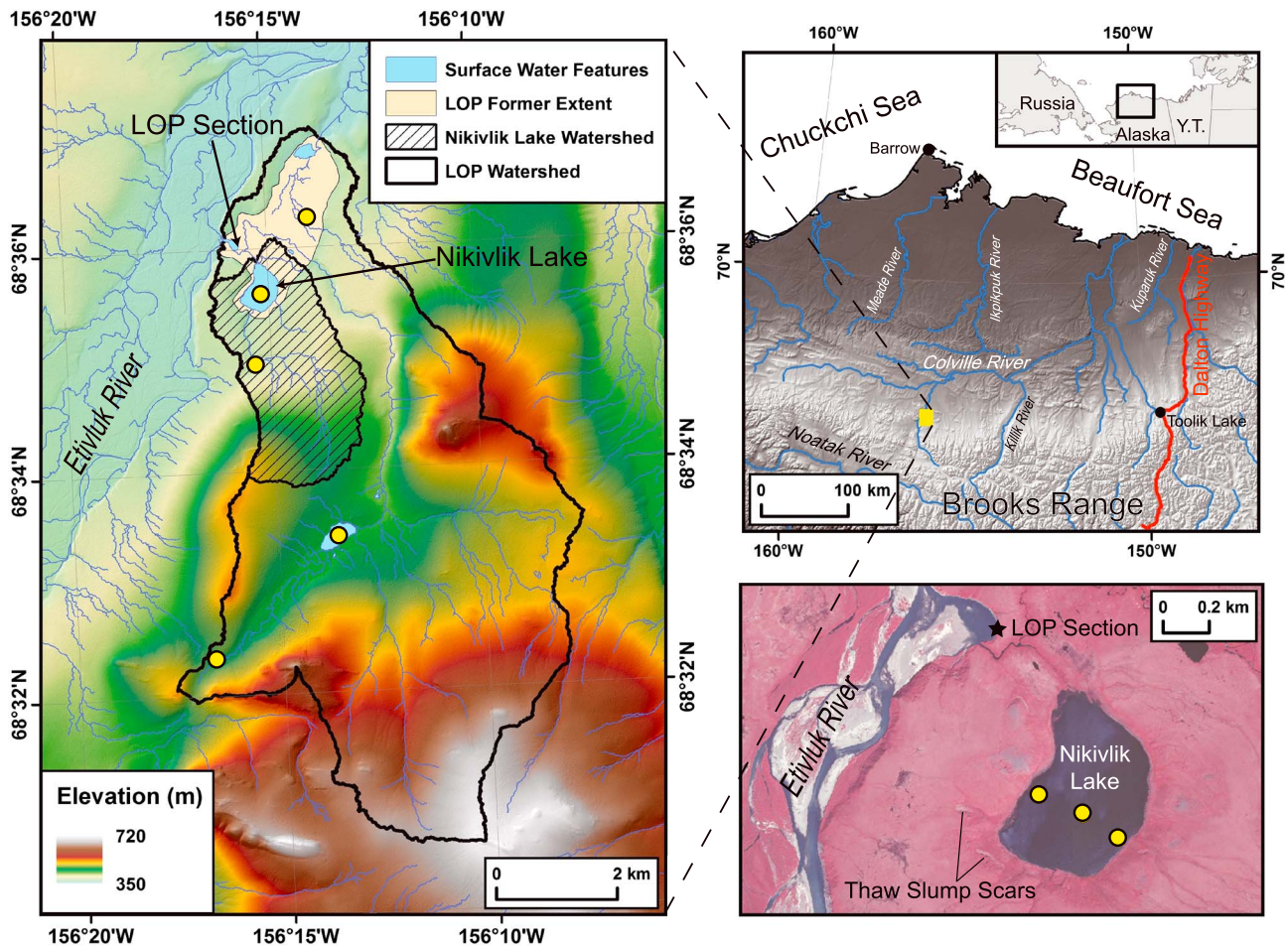
Figure 1. Location and extent of the former Lake of the Pleistocene (LOP) and modern Nikivlik Lake with their respective watersheds outlined. Sampling sites are referred to in the text. Yellow dots are the locations where surface sediment lake cores and inlet water POC were collected.

warming triggered widespread thermokarst in northern Alaska, hillslopes delivered enormous sediment loads to major rivers and caused floodplain aggradation [*Mann et al.*, 2010]. Such wholesale landscape change in the future would impact development projects and the management of freshwater and marine resources in the Arctic.

Despite these potential risks, the long-term perspectives on the rates and vulnerabilities of permafrost thaw and OC release have rarely been pursued [*Walter et al.*, 2007; *Mann et al.*, 2010; *Reyes et al.*, 2010]. This lack of context is a critical knowledge gap because the links between climate, permafrost thaw, and C release involve complex biophysical processes that are difficult to predict and understand by using short-term observations [*Heimann and Reichstein*, 2008; *Schaefer et al.*, 2011; *Vonk and Gustafsson*, 2013]. Moreover, without a prehistoric baseline describing the normal rates of thaw and release, we cannot recognize whether recent warming has already affected permafrost vulnerability. In this study, we utilize paleo-records of past OC release from an arctic watershed underlain by permafrost to establish how OC release was affected during past climate fluctuations. In turn, we determine if present release rates are exceptional relative to the prehistoric norm.

The watershed whose OC dynamics are reconstructed here is representative of numerous tundra watersheds in the Arctic Foothills of northern Alaska. But it does have one unique feature: A wide cross section of the former lake bed is now exposed, which enables exceptional access to the ancient sedimentary record. Using material from the exposed deposits, we generate a time series of ^{14}C age-offsets encompassing prehistoric periods of warming and cooling from the latest Pleistocene (beginning 14.5 ka) through much of the Holocene (last 11.7 ka). As detailed in section 3 below, a ^{14}C age-offset is the difference between the "true" age of sediment
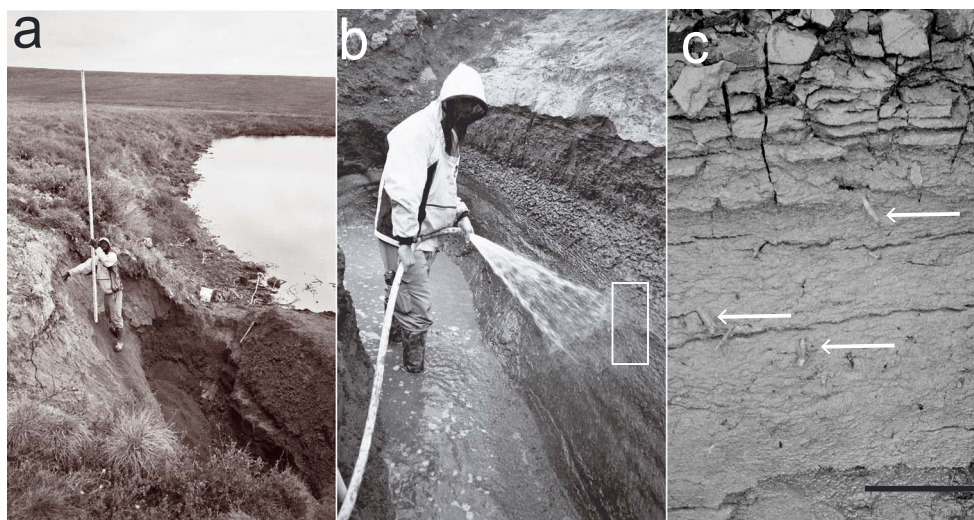
Figure 2. Lake of the Pleistocene (LOP) section, July 2012. (a) Describing stratigraphy at the LOP section. The Etivluk River at right. (b) Pressure washing the frozen, intact face of the LOP section before sampling. White box is enlarged in Figure 2c. (c) Close-up of willow twigs (white arrows) embedded in the transition from Units 3 to 4. Scale bar is 0.1 m.

deposition and the apparent ^{14}C age of the lake sediment, with the offset being caused by contributions of aged OC from the watershed soils and permafrost. Known periods of past climate change including rapid climate oscillations during deglacial periods (16 to 10 ka), gradual cooling over the Neoglacial period (last 6 ka), and warming since A.D. 1850 together provide an opportunity for testing the sensitivity of OC release to a changing climate in the Arctic.

2. Study Area and Paleoclimate Background

The genesis and history of the study lake, as well as the climate, permafrost, soils, geomorphology, and vegetation in its watershed, have determined how OC is stored in the watershed, imported to the lake, and how it is likely to migrate within the lake basin. "Lake of the Pleistocene" (informal name; LOP; 68°36′2.77″N 156°15′40.75″W; 362 m elevation) is a partially drained lake basin (Figure 1). LOP formed at least 40 ka in an alas valley (thermokarst-formed valley) tributary to the Etivluk River, 60 km north of the crest of the Brooks Range in the Arctic Foothills region of the North Slope of Alaska [*Mann et al.*, 2002]. LOP was dry during the last glacial period (~25 to 16 ka) but then refilled and resumed lacustrine sedimentation around 15 ka [*Mann et al.*, 2002]. During this period of lake refilling, shoreline expansion likely took place through the process of thermokarst erosion [*Mann et al.*, 2002]. Around 5 ka, the lake partially drained when the Etivluk River changed its course and eroded through its northwestern sill (Figures 1 and 2). Further channel migration has resulted in a cut bank exposing a 200 m wide cross section of the old lake bed of LOP (Figures 1 and 2). At its full extent, LOP is estimated to have covered an area of ~3 km^2 with an estimated watershed area of ~41 km^2 (See section 5 for details of former lake and watershed delineation). The deepest part of LOP would have been anywhere from ~5 to 10 m deep based on the digital elevation model of the former basin. Part of this basin was not drained by the encroaching river around 5.6 ka and today contains a shallow (~2 m deep) lake ("Nikivlik Lake") covering ~0.32 km^2. In recent years this lake likely does not freeze to the bottom sediments based on remote sensing inferences of ice thickness elsewhere in the region [*Grunblatt and Atwood*, 2014] and lake ice thickness measured elsewhere in the Arctic foothills (C. Arp et al., unpublished data, 2014). Nikivlik Lake is fed by a ~6.15 km^2 portion of the former LOP watershed. The watersheds of these lakes are underlain by continuous permafrost and have not been directly affected by glaciation since the mid-Pleistocene [*Hamilton*, 2001]. In a nearby river bluff exposure, glacial outwash likely from the Anaktuvuk or Sagavanirktok River glaciations [*Hamilton*, 2001] is capped by a ~3 m thick layer of loess and sand sheet sediment. Syngenetic and epigenetic ice wedges as well as sill ice (horizontal lenses accumulating at the bottom of old active layers) penetrate these Quaternary deposits. This subsurface stratigraphy is probably representative of the permafrost underlying most of the LOP watershed.

The development of organic-rich, Holocene soils on top of well-drained Pleistocene soils in the Arctic Foothills is the foundation of many of the region's signature environmental and physical attributes today. Relatively warm and wet conditions at the end of the last glacial period enhanced vegetation productivity causing a surplus of organic material to accumulate onto increasingly moist soils [*Jones and Yu*, 2010]. Starting around 9 ka, thickening organic layers on the ground surface insulated the permafrost from summer thaw, held more water, reduced cation exchange, and favored acid-tolerant, peat-forming plants [*Mann et al.*, 2002; *Oswald et al.*, 2003]. Today, surface soil organic layers (soil organic horizons <0.3 m thick) and peats (soil organic horizons >0.3 m thick) are widespread on the modern landscape. These surficial deposits store large amounts of OC, insulate the underlying permafrost from warming air temperatures, and hence protect the underlying mineral layers from thermal and mechanical erosion [*Bockheim et al.*, 1996; *McNamara et al.*, 1998; *Baughman*, 2013].

Today, vegetation in the LOP watershed is primarily moist acidic tundra representative of the Arctic Foothills region. Moist acidic tundra is characterized by tussock-forming sedges (*Eriophorum vaginatum* L.) growing on both low-relief lowlands and on poorly drained uplands [*Raynolds et al.*, 2005; *Walker et al.*, 2005]. Riparian corridors, lake shorelines, snow drift sites, water tracks, and gullies are lined with willow shrubs and occasional birch shrubs [*Raynolds et al.*, 2005; *Walker et al.*, 2005].

The Arctic Foothills experienced the same rapid climate warming and cooling events at the end of the last glacial period that occurred throughout the circumarctic region [*Miller et al.*, 2010]. The expansion of cottonwood trees (*Populus balsamifera* L.) beyond their present limit, widespread peatland initiation, increased thermokarst, and aggrading floodplains indicate that the summer temperatures warmed rapidly amounting to around ~2–3° Celsius (C) of warmer-than-present summer temperatures starting around 14.5 ka [*Mann et al.*, 2002, 2010]. These warmer-than-present conditions persisted for at least 5 ka, during a time of greater summer insolation in the Northern Hemisphere [*Kaufman et al.*, 2004], but were interrupted by a ~1200 year-long return of colder-than-present and drier conditions during the Younger Dryas episode (12.9 to 11.7 ka) [*Alley*, 2000; *Mann et al.*, 2010].

Over the last 6 ka, summer temperatures have gradually cooled in the Brooks Range [*Calkin*, 1988; *Anderson et al.*, 2001; *Badding et al.*, 2012]. The Little Ice Age is well expressed in Arctic Alaska by changes in latewood densities in tree rings [*Anchukaitis et al.*, 2013], episodes of moraine building [*Calkin*, 1988; *Badding et al.*, 2012], and paleolimnological reconstructions of temperature [*Anderson et al.*, 2001; *Bird et al.*, 2008]. Most studies agree that the Little Ice Age ended around A.D. 1850 followed by gradual warming [*Bird et al.*, 2008; *Kaufman et al.*, 2009; *Badding et al.*, 2012; *Anchukaitis et al.*, 2013], and then more rapid warming beginning in the mid-twentieth century [*Hinzman et al.*, 2005]. Today, average summer temperatures in the Eastern Brooks Range are roughly 1.3°C warmer than the average over the last millennium [*Anchukaitis et al.*, 2013]. Mean summer temperatures rose by ~1°C on the North Slope over the latter half of the twentieth century [*Stafford et al.*, 2000].

3. Methodological Background

3.1. ^{14}C Age-Offsets

The paleoarchive of permafrost OC we explore here involves shifts in the apparent ^{14}C age of OC deposited in a lake over time. Accumulating lake sediment often preserves a long-term time series of OC input from the surrounding watershed. Terrestrial-derived dissolved and particulate organic carbon (DOC and POC, respectively) enter lakes through leaching and erosion of OC that has spent varying periods stored in soils and/or permafrost [*Guo et al.*, 2007; *Raymond et al.*, 2007; *Gustafsson et al.*, 2011]. Millennial-aged DOC has been observed in rivers in Arctic Alaska [*Guo et al.*, 2007], and high rates of DOC flocculation and sedimentation have been observed in high-latitude lakes [*Wachenfeldt and Tranvik*, 2008]. POC has been identified as the oldest OC fraction in Arctic Alaska rivers [*Guo et al.*, 2007] and the Yukon River [*Guo and Macdonald*, 2006] and can readily settle in still water environments and become added to lake and marine sediments. Older POC occurs downstream from thaw-driven mass movements in the Canadian Arctic [*Lamoureux and Lafrenière*, 2014]. As a result of these aged carbon inputs, the ^{14}C ages of OC deposited in lake, marine, and floodplain sediments give an overestimate of the depositional ages of sediment horizons because this OC was stored in the surrounding soils and/or permafrost prior to being reworked [*Abbott and Stafford*, 1996; *Vonk et al.*, 2010].

Radiocarbon age-offsets in lake sedimentary sequences are determined by the ^{14}C age differences between the bulk sediment comprising SOC reworked from the watershed and associated macrofossils derived from terrestrial plants. In contrast to the mixed ages of the different OC components in a bulk sample of lake sediment, fragments of terrestrial plants that were growing around the lake (leaves, twigs, seeds, and other plant parts, collectively called plant macrofossils) are often incorporated into lake sediment immediately after they die. Thus, the ^{14}C age of a terrestrial plant macrofossils records the true depositional age of the sediment horizon in which it occurs [*Oswald et al.*, 2005], whereas the ^{14}C age of the bulk sediment in the same sedimentary layer is usually older because it integrates the ages of OC derived from a mix of contemporaneous and aged sources [*Wolfe et al.*, 2004].

Interpreting an age-offset record requires an assessment of the provenance and ^{14}C age of all organic matter sources potentially contributing to the bulk sediment deposited in a lake basin. Age-offsets can be complicated by within-lake primary productivity (autochthonous organic matter) that assimilates C from modern atmospheric CO_2 dissolved in the lake, or from that of ancient dissolved inorganic carbon (DIC; sum of CO_2, HCO_3, and CO_3 in dissolved form) derived from either soil or sediment respiration [*Algesten et al.*, 2005] or from dissolution of carbonate bedrock [*Pons et al.*, 1998]. Because submerged macrophytes take up DIC from lake water, their ^{14}C ages provide a proxy for the age of aqueous DIC mixture and for the ^{14}C age of autochthonous OC contributing to age-offset records. The proportion of terrestrial- versus aquatic-derived organic matter can further be constrained with bulk sediment C:N, and δ^{13}C values [*Meyers and Ishiwatari*, 1993]. In general, arctic lake sediment with higher C:N values (>10) and relatively high δ^{13}C ($>-30‰$) values imply significant contributions from terrestrial organic matter to lake sediment [*Meyers and Ishiwatari*, 1993].

Lake-level changes can also complicate the interpretation of age-offset records because organic matter deposited on the lake bottom can be reworked when the water level rises or falls. This can cause the redistribution of aged OC to other parts of the lake, influencing age-offset signals there [*Håkanson and Jansson*, 2002]. The depth of wave base in a lake, and its influence on sedimentation patterns within a basin, can be estimated through wave base modeling and observations of recent sediment deposition for a given site [*Håkanson and Jansson*, 2002]. Further, a record of the timing of past lake-level changes inferred from sedimentology transitions can test whether changes in an age-offset record are influenced by within-lake or shoreline sediment reworking. In the Arctic, the age-offsets of OC deposited in deep water below wave base in soft water lakes with well-mixed water columns are mainly influenced by aged allochthonous OC sources derived from the watershed [*Abbott and Stafford*, 1996].

Previous studies that have used ^{14}C age-offsets in lake sediment records to infer changes in OC imported from watershed soils to lakes had different interpretations of what drove age-offsets. In Iceland over the last 2 ka, increased age-offsets occurred during boughts of cold, windy climate episodes, which limited vegetation and made SOC available for aeolian erosion [*Geirsdóttir et al.*, 2009]. In Britain, age reversals occurred in the ^{14}C ages of bulk sediment deposited in lakes during the mid-Holocene elm decline when forest soils were deeply eroded [*Edwards and Whittington*, 2001]. By measuring organic matter deposition over the last several decades in a subarctic Swedish lake, *Vonk et al.* [2012] correlated changes in sediment age-offsets to an increase in the amount of peat eroded from the watershed in response to warming climate. Although the causative process of the age-offset varied in each of these cases, the age-offset record provided a proxy for the amount and age of SOC laterally transferred from watershed to lake.

Arctic soils have unique processes of SOC storage important for interpreting age-offsets there. SOC that evades degradation and is stored in the active layer may still be respired later, reworked by leaching or erosion, or incorporated into the permafrost [*Billings*, 1987]. OC can pass through the active layer into permafrost by a number of different processes including vertical mixing by cryoturbation that redistributes organic matter in the soil column [*Bockheim*, 2007], or aggradation of permafrost in response to organic matter accumulating on the ground surface [*Bockheim et al.*, 1996]. Additionally, though rare on the landscape today, rapid deposition of aeolian sediments during the ice age incorporated large amounts of SOC into permafrost in the form of *yedoma*, ice-rich deposits of organic-rich silt and fine sand [*Kanevskiy et al.*, 2011; *Schirrmeister et al.*, 2012].

The stability of SOC in the Arctic is strongly influenced by permafrost thaw, which in turn plays an important role in most periglacial geomorphic processes. Enhanced stream erosion, mass movements, and active layer deepening can all involve the thawing of permafrost containing aged OC [*French*, 2010]. When this permafrost thaws, the aged OC is released to streams, and some of it is eventually deposited in lake basins. Therefore,

a time series of age-offsets provides a proxy for the changing input of aged OC into the lake basin, which in turn reflects the amount of permafrost thaw in the watershed. Climate warming that triggers permafrost thaw also enhances mobilization of OC stored in the active layer through leaching and erosion ending up in downstream lakes [*Frey and McClelland*, 2009]. Therefore, by comparing a time series of ^{14}C age-offsets with known periods of climate change in the past, we can gauge the sensitivity of OC stored in tundra soils and permafrost to release triggered by warming and cooling of regional climate.

3.2. Ramped-Temperature [14]C Dating

Although age-offsets are a proxy for inputs of aged OC into lake basins, they do not identify the sources and nature of OC released from the watershed. For this purpose, we employed the Programmed Temperature Pyrolysis/Combustion System ^{14}C dating (ramped-temperature ^{14}C) technique that has also been used to constrain geologic and pedogenic OC sources exported by the Mississippi and Ganges Rivers [*Rosenheim and Galy*, 2012; *Rosenheim et al.*, 2013a, 2013b], to identify the likely OC sources influencing age-offsets in the Southern Ocean [*Rosenheim et al.*, 2008] and to the Colville River estuarine system on the North Slope of Alaska [*Schreiner et al.*, 2014]. To determine the ^{14}C sources that contribute to sedimentary OC in depositional environments, the sediment sample is sequentially heated and the resulting CO_2 gas is trapped and dated to provide a continuum of ^{14}C ages for a given sample. [14]C ages in the low-temperature fractions typically incorporate very unstable or fresh material such as autochthonous algae [*Rosenheim et al.*, 2008]. Higher temperature ^{14}C ages are often older because this recalcitrant organic matter has been exposed to decomposition for a longer period of time than more labile, fresh compounds. Examples of compounds that are expected in the higher-temperature fractions are terrestrial vascular plant material that has undergone decomposition and is preserved in terrestrial soils. Comparing the gas sample ages to the true age of deposition results in multiple age-offsets that constrain what OC pools are integrated in the bulk age-offset. A thermal stability index, calculated as the proportion of OC in a sample that is combusted at lower temperatures, is used to compare organic matter quality in different bulk sediment samples [*Plante et al.*, 2009].

4. Methods

4.1. Field Sampling

4.1.1. Sources of Lake Sediment OC Today

We collected surface sediment samples from five lakes and ponds in the LOP watershed using a Bolivia piston corer and a Russian peat corer. A single core was taken from the deepest water in each of the four unnamed ponds (Figure 1). In addition, three cores were taken from Nikivlik Lake along a depth transect (0.9, 1.3, and 1.7 m water depth) to observe the variation in lithology and organic geochemistry in different depositional settings (Figure 1). Neither the Russian nor Bolivia corers could penetrate deeper than 0.3 m into the Nikivlik Lake sediments using human power alone. Sediment from the uppermost 0.02 m of all cores was sampled in the field for bulk ^{14}C dating, loss on ignition (LOI), as well as stable carbon isotope analysis and elemental (organic carbon and nitrogen) analysis (described below). We sampled surface sediment where it was undisturbed by coring and had an intact sediment-water interface. Inlet water from each lake, and outlet water from Nikivlik Lake, was filtered through previously baked (500°C) 0.7 μm glass fiber filters GF/F (Whatman) to obtain POC for ^{14}C dating (PO[14]C) and for elemental and stable isotope analysis. Two rooted and living aquatic macrophytes that were completely submerged in two different lakes (Nikivlik Lake and the uppermost unnamed pond) were also collected for ^{14}C dating.

4.1.2. Sampling the LOP Section

An 8 m wide swath of the former sediment bed of LOP (Figure 1) was exposed by digging with hand tools and pressure washing and then described and sampled during the summers of 2011 and 2012 (Figure 2). Several other test pits were dug on either side of the main exposure to confirm our sampling site was representative of the larger exposure. Sediment sampling and descriptions were conducted on a vertical and recently thawed sediment face that was undisturbed by cryoturbation and slumping. A surveying level and stadia rod were used to measure the relative heights of different sediment horizons and samples. Grain size was qualitatively assessed, and sediment lithologies were described in the field and compared with those found at different depths in Nikivlik Lake today to infer lake-level changes in the past. Volumetric sediment samples were taken throughout the profile for dry bulk density, LOI, as well as elemental and stable isotope analysis. Paired ^{14}C age-offset samples were taken by sampling terrestrial plant macrofossils along with the sediment matrix

immediately surrounding them (Figure 2c). In practice, this meant collecting a 1 cm^3 block of the fine-grained lake sediment enclosing each terrestrial plant macrofossil intended for ^{14}C dating.

4.2. Laboratory Analysis and ^{14}C Dating

LOI was performed on sediment samples by measuring the mass of sediment before and after heating to 550° and 1050°C for 5 and 3 h, respectively (LOI$_{550°}$ and LOI$_{1050°}$) [*Heiri et al.*, 2001]. All sediment samples analyzed for carbon and nitrogen percent and stable carbon isotopes were acidified in 10% HCl overnight to remove inorganic carbon and then washed and decanted with de-ionized water until reaching a pH of 5. Freeze-dried sediment was then analyzed using a Costech ESC 4010 elemental analyzer interfaced via a ThermoConflo III to a Thermo Scientific Delta V isotope ratio mass spectrometer. All stable carbon isotope values are expressed relative to Vienna Pee Dee belemnite in delta notation (i.e., δ^{13}C values) in per mil values (‰). The analytical precisions (defined here as 1 standard deviation calculated from eight analyses of peptone as an internal laboratory standard) for %C, %N, and δ^{13}C were 1.0%, 0.4%, and 0.2‰, respectively.

Twig and leaf ^{14}C samples (terrestrial plant macrofossils from willow and birch shrubs) were given acid–base–acid rinses typical for ^{14}C plant sample preparations [*Brock et al.*, 2010]. Bulk sediment to be ^{14}C dated was washed through a 180 μm diameter sieve to exclude any large plant macrofossils. The sample was then acidified with 10% HCl to remove inorganic carbon and then washed and decanted with de-ionized water until the solution reached a pH of 5. The filters used for PO^{14}C sampling were freeze dried, reweighed, and acidified as described above. All ^{14}C samples were analyzed on an accelerator mass spectrometer (AMS) at the National Ocean Sciences Accelerator Mass Spectrometer facility in Woods Hole, Massachusetts, or at the Beta Analytic Laboratory in Miami, Florida.

4.3. Ramped-Temperature ^{14}C

Using the methods of *Rosenheim et al.* [2008], we ^{14}C dated the CO$_2$ released during ramped-temperature treatments of bulk sediment samples from five different stratigraphic units in the LOP section, and one sample of near-surface sediment from Nikivlik Lake. Prior to ramped-temperature treatment, bulk sediment to be ^{14}C dated was acidified (as described above) and washed through a 500 μm diameter sieve. Each gas sample was graphitized, and targets were analyzed by AMS at the National Ocean Sciences Accelerator Mass Spectrometry facility. A portion of all gas samples being graphitized for ^{14}C analyses were kept for stable carbon isotope analysis to calibrate ^{14}C ages for varying thermodynamic fractionation occurring at different temperatures [*Reimer et al.*, 2013].

4.4. Data Analysis

4.4.1. LOP Extent, Watershed Delineation, and Wave Base Modeling in Nikivlik Lake

The delineation of the former extent of LOP is based on stratigraphic surveys of exposed sediments [*Mann et al.*, 2002], analysis of color-infrared orthophotography (2.5 m spatial resolution), and analysis of a digital terrain model (5 m spatial resolution) derived from Interferometric Synthetic Aperture Radar (IfSAR) data. The IfSAR data were also used to automatically delineate the watershed area by using the hydrology toolbox available in ArcGIS v. 10.1®. To summarize briefly, all sinks were filled in the IfSAR digital terrain model, flow paths and flow accumulation values were derived, and pour points were placed at junctions between the flow paths and the former extent of LOP.

We used the model of *Carper and Bachmann* [1984] to estimate the depth of wave base at coring locations in Nikivlik Lake. Input to the model included the wind speed and wind direction recorded at the Ivotuk climate station (25 km to the east of LOP) during the ice-free season (~1 June to 1 September) between A.D. 1998 and 2006, and the effective fetch distance at each coring location.

4.4.2. Age-Depth Modeling and Stratigraphic Units in the LOP Section

We used the BACON ("Bayesian accumulation histories") modeling package in Rstudio software [*Blaauw*, 2010] to build a true age-depth model for the LOP section based on the ^{14}C ages of terrestrial plant macrofossils. All ^{14}C ages reported were calibrated using the IntCal13 curve [*Reimer et al.*, 2013]. This age-depth modeling method divided the sediment stack into one hundred thirty 0.03 m thick sections and went through several million Monte Carlo iterations to estimate the accumulation rate of the sediment using the calibrated macrofossil ^{14}C ages from multiple layers. The bulk sediment ages were modeled using a cubic spline interpolation model in the CLAM ("classical, non-Bayesian age-depth modeling") package in Rstudio software [*Blaauw*, 2010], which took into account the age reversals observed in the bulk sediment chronology that are

Table 1. Wave Base Modeling Results[a]

Wind Direction	Effective Fetch (m)	Average Wave Base (m)	Max Wave Base (m)
0.9 m Deep Core Site			
North	508	0.36	**1.12**
Northeast	153	0.30	0.89
East	36	0.11	0.33
Southeast	32	0.07	0.29
South	52	0.13	0.55
Southwest	218	0.52	**1.42**
West	469	0.52	**1.79**
Northwest	453	0.35	**1.32**
1.3 m Deep Core Site			
North	93	0.17	0.49
Northeast	467	0.51	**1.54**
East	462	0.37	1.15
Southeast	412	0.24	1.00
South	293	0.30	**1.28**
Southwest	214	0.51	**1.41**
West	80	0.23	0.75
Northwest	58	0.13	0.48
1.7 m Deep Core Site			
North	512	0.36	1.12
Northeast	374	0.46	1.38
East	259	0.28	0.87
Southeast	217	0.18	0.73
South	262	0.28	1.21
Southwest	284	0.59	1.62
West	320	0.44	1.49
Northwest	262	0.27	1.02

[a]Bold depths are where modeled wave base is below depth of water.

potentially important for changes in age-offsets through time. The interpolated age-offset was constructed by subtracting the best fit (median age estimate) of the macrofossil model from the best fit of the bulk sediment spline model estimated for the same depth. Individual age-offsets were calculated by subtracting the macrofossils median age and error (2σ calibrated age range) from the median and error of the bulk sediment age from the same layer. We refer to two age-offset values below: (1) individual age-offsets of a given layer determined by the age difference between the two dated samples (terrestrial plant macrofossil and bulk matrix) and (2) modeled age-offsets where the interpolated true age of a given layer is subtracted from the interpolated bulk sediment age of the same layer.

4.4.3. Ramped-Temperature Analysis

We modeled the normalized ages of the ramped-temperature gas samples against the average temperature in which they were combusted using a general additive model. Normalized ages were estimated by

$$^{14}C_N = (x - \mu)/\sigma \tag{1}$$

where $^{14}C_N$ is the normalized age, x is the calibrated ^{14}C age of the individual gas sample, μ is the mean of all gas sample ages from the sediment horizon, and σ is the standard deviation of all the gas sample ages analyzed from that sediment horizon. Normalizing allows all gas samples to be compared with temperature together in order to model patterns of how relative age within a bulk sediment sample is related to thermal stability.

We calculated a thermal stability index for each sample analyzed by ramped-temperature techniques using the approach of *Baffi et al.* [2007]:

$$TI = CO_2(410 - 600°C)/CO_2(180 - 410°C) \tag{2}$$

where TI is the thermal stability index and the two CO_2 variables are how much CO_2 the sample produced during heating in these two temperature ranges.

We used the standard deviation of within-sample gas ^{14}C ages to assess the age ranges of OC sources to individual bulk sediment samples. We used uncalibrated ^{14}C ages because using calibrated dates may cause larger age ranges from some time periods but not others. This disparity originates from age plateaus and age reversals from some time periods in the ^{14}C calibration curve [*Reimer et al.*, 2013].

The total OC deposited in LOP was calculated by

$$g\, OC/m^2/yr = (\%OC/100 \times kg/m^3) \times (m/yr) \tag{3}$$

where kg/m^3 is the dry bulk density of the sediment and m/yr is the accumulation rate of sediment per year.

We estimated the proportion of OC deposited in LOP per meter per year that was "ancient," which we define as >1.0 ka old at the time of deposition. Using the proportion of CO_2 in the ramped-temperature ^{14}C ages
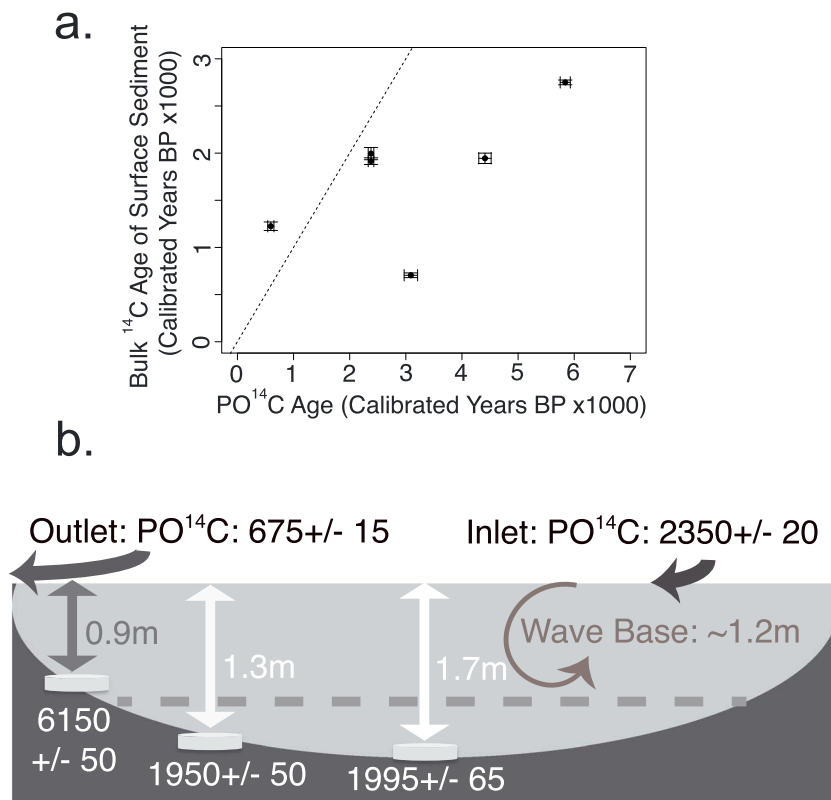
a.

b.

Figure 3. (a) Scatterplot showing particulate organic carbon radiocarbon age (PO[14]C) of inlet water and age of surface sediments in LOP watershed lakes excluding the nearshore deposit in Nikivlik Lake (the core sampled from 0.9 m water depth). The dotted line represents the 1:1 relationship and illustrates that all but one lake has older OC entering through the inlet than is being deposited in the sediment. (b) PO[14]C ages of surface sediment samples and entering and exiting Nikivlik Lake.

that was >1 ka older than the 95% upper limit of the macrofossil true age from that same layer, we estimated the proportion of the OC deposited in LOP that was ancient at seven different time periods in the past and assigned these proportions to all depths in their respective sedimentary units. Rates of ancient OC deposition was calculated by

$$g \text{ ancient OC/ } m^2/yr = (g \text{ total OC/m/yr}) \times (mg\ CO_2 > 1\ ka\ /\ mg\ total\ CO_2) \tag{4}$$

where total OC/m^2/yr is calculated from equation (3) and mg CO_2 is the mass of CO_2 in the sample that resulted in bulk sediment combustion, while the mg $CO_2 > 1$ ka is the mass of CO_2 that was greater than 1 ka older than the true age of the same layer.

5. Results

5.1. Nikivlik Lake Lithofacies

According to the wave base model, surface sediment along the depth transect where our cores were taken in Nikivlik Lake was frequently disturbed by wind waves at water depths <1 m, occasionally disturbed at water depths between 1.0 and 1.4 m, and rarely disturbed at depths >1.4 m (Table 1). Nearshore lake sediment in <1.0 m water depth is mainly coarse sand and is organic poor (LOI$_{550°}$ <2.0%; Nikivlik Lake organic geochemistry data not shown), with low C:N values (<8). Between 1.0 and 1.2 m water depths, silty sediment contains storm-related laminae each consisting of sand grading upward to silt, clay, and then organic debris including willow leaves and twigs. This zone of deposition had relatively high organic matter content (LOI$_{550°}$ >10.0%) and C:N values (>10). Nikivlik Lake sediment in >1.2 m water depth was composed of massively bedded fine silt with ~8.0% organic matter (LOI$_{550°}$) and moderate C:N values (8–10). All surface sediment sampled from Nikivlik and other modern lakes as well as the LOP sediments had <1.5% dry weight of inorganic carbon based on the LOI$_{1050°}$ method.
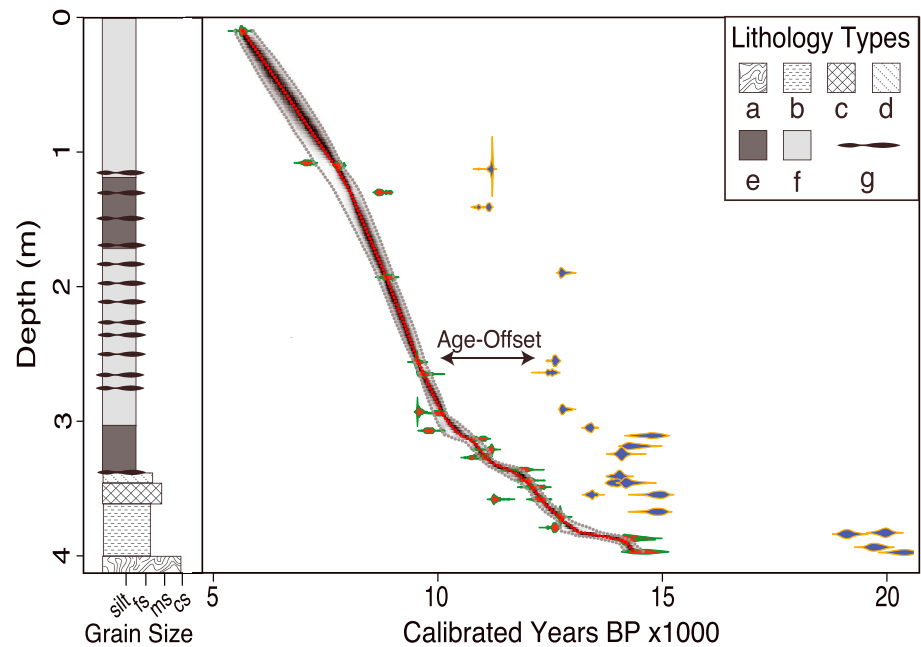
Figure 4. Sediment stratigraphy and age-depth modeling based on individual ^{14}C ages and interpolated ages in the LOP section. Plant macrofossil ages are shown in red with green outline. Bulk sediment ages are shown in purple with orange outline. Lithologic units are as follows: (a) gray and oxidized, coarse sand with pillow-like intrusions of sandy gravel from the base of section and occasional clods of terrestrial peat; (b) dark gray, sandy silt with medium organic content; (c) medium gray, silty sand with abundant terrestrial organic matter and gastropods; (d) light tan silt with low concentration of organic matter; (e) dark brown, organic-rich silt that has a massive structure with rare laminae; (f) light brown, organic-rich silt; and (g) organic-rich sediment with numerous leaf and twig layers enclosed within silt and clay laminae deposited in storm/poststorm, fining-upward sequences.

5.2. [14]C Ages of OC in Streams and Lakes Today

The bulk ^{14}C ages of surface sediment samples from deep water cores (water depth >1.0 m; $n = 5$ different lakes/ponds) ranged from 0.7 to 2.7 ka (Figure 3). Surface sediment ages from two cores taken from 1.3 to 1.7 m water depth in the depositional zone (a zone rarely affected by wave base in Nikivlik Lake) had overlapping ages (both rounded to 2.0 ka median ages; Figure 3b). Because this sediment is undisturbed and represents recently deposited sediment, it serves as the age-offset estimate for the watershed today (2.0 ka). A shallow water surface sediment sample (0.9 m water depth) composed of coarse, gravelly sand in the erosional zone frequently disturbed by wave base was much older at 6.2 ka (Figure 3b).

POC samples collected at stream mouths in lake inlets and in lake water had ^{14}C ages ranging from 0.5 to 5.9 ka ($n = 5$; Figure 3a). The POC entering four of the five study lakes was significantly older than the age of the surface sediments in that lake (Figure 3a). The POC sampled from the inlet water entering Nikivlik Lake was 2.4 ka, whereas POC in the Nikivlik Lake outlet stream dated to 0.7 ka (Figure 3b). The ^{14}C content of submerged macrophytes was influenced by the global bomb-^{14}C spike as shown by their fraction modern values of 1.0211 ± 0.0024 and 1.0253 ± 0.0036 (supporting information Table S1). As a result, the DIC pool for autochthonous productivity is at near-modern levels, uninfluenced by ancient C from carbonate dissolution or heterotrophic respiration.

5.3. Organic Geochemistry, Lake-Level History, and Age-Offsets in LOP

Distinct lithological and geochemical changes in the LOP section indicate fluctuations in the provenance (C:N, δ^{13}C values) and age (^{14}C age-offset) of organic matter deposited as lake sediment in the LOP basin between 14.4 and 7.0 ka (Figures 4 and 5). Evidence for changes in water levels comes from distinct sedimentological units that are analogous to those found at different depths in Nikivlik Lake today. Twenty-five ^{14}C dates on twig and leaf samples are the basis for the age-depth interpolation of the unit boundaries in the LOP section (Figures 4 and 5).
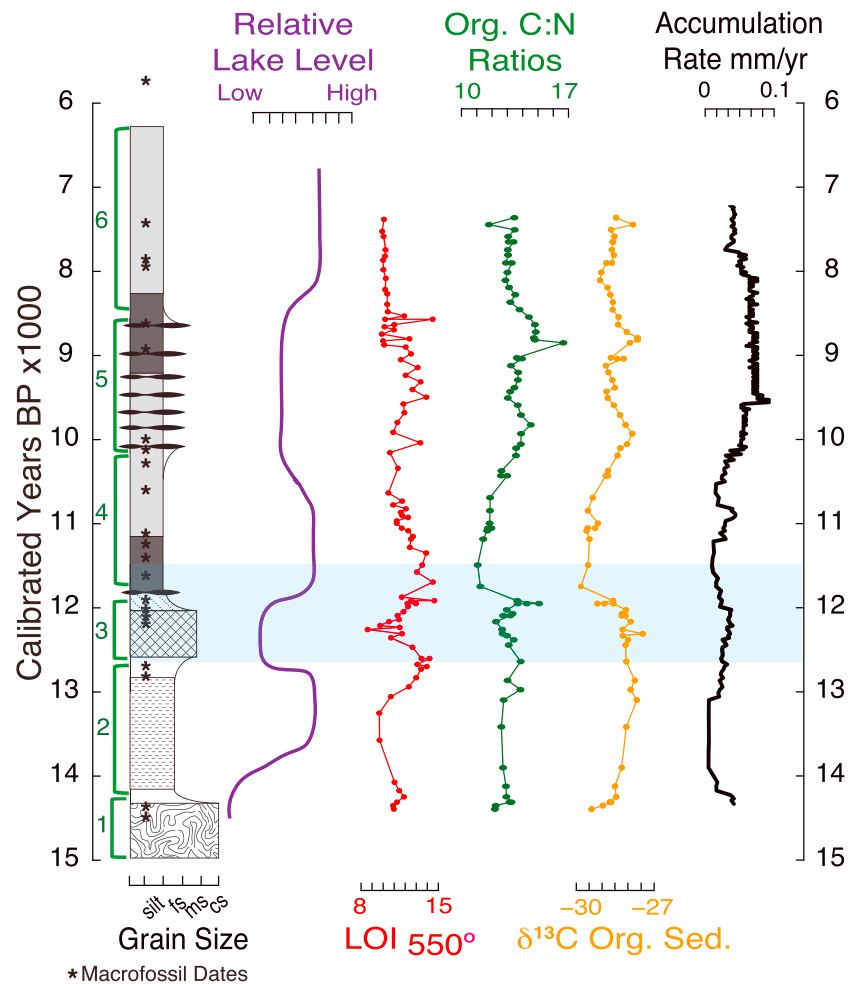
Figure 5. Organic geochemistry data from the LOP section plotted against the calibrated age-depth model of macrofossil ages (each date noted by black stars in the lithology column). Lake-level changes are interpreted from sedimentary structures in the LOP section in combination with their modern analogs along a water depth transect in Nikivlik Lake today. Sedimentary units shown by green boxes on left. The Younger Dryas chronozone is shaded in blue.

5.3.1. LOP Sediment Units

5.3.1.1. Unit 1: Disturbed, Nearshore Deposit, >14.4 ka (Lythotype a in Figure 4)

Prior to 14.4 ka, the sediment deposited in the lake basin at the site of the LOP section consisted mainly of coarse sand and small pebbles along with allochthonous peat clods (Figures 4 and 5). Low organic content (2.7% mean $LOI_{550°}$), very high age-offsets (8.0 ka; n = 2; not shown), macrofossil age reversals, and very low organic C:N values (<10) together suggest that this unit was deposited in shallow water in a setting analogous to the nearshore deposit in Nikivlik Lake (0.9 m water depth) that is affected by high wave energy today. The peat clods and very high age-offsets indicate that this unit represents thermokarst shoreline erosion from the lake being refilled after the arid full glacial period.

5.3.1.2. Unit 2: Undisturbed, Deep Water, Medium Organic Content Lake Deposit, 14.4–12.4 ka (Lythotype b in Figure 4)

Finer-grained sediment with relatively high C:N values (12.4 mean) and δ^{13}C values (−28.4‰ mean) accumulated between 14.4 and 12.4 ka in the LOP basin (Figures 4 and 5). This unit was composed of sandy silt and is analogous to the deep water Nikivlik Lake deposits that are currently below wave base.

5.3.1.3. Unit 3: Undisturbed, Shallow Water, Organic-Poor, Lake Deposit, 12.4–11.9 ka (Lythotypes c and d in Figure 4)

Organic-poor (10.8% mean $LOI_{550°}$), silty sand with relatively high C:N values (12.7 mean) and δ^{13}C values (−28.2‰ mean) was deposited between 12.4 and 11.9 ka (Figures 4 and 5). This unit has no depositional
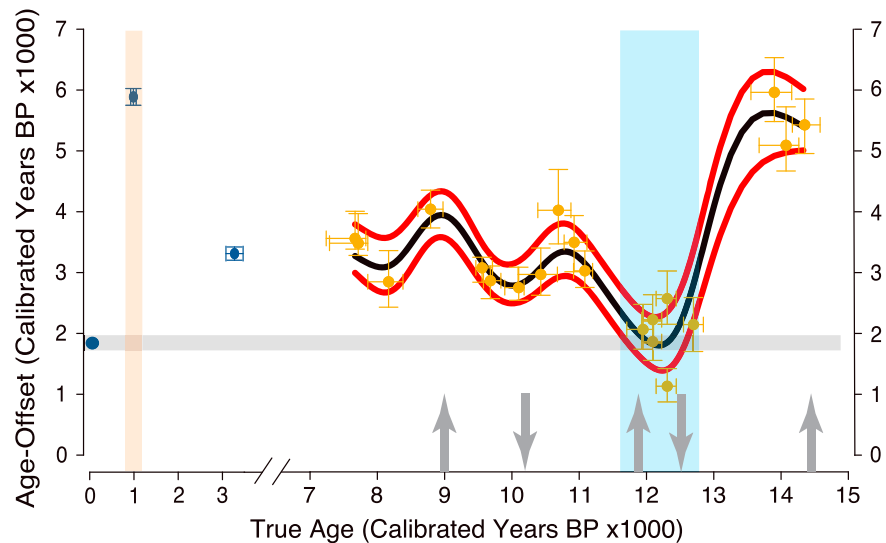
Figure 6. Summary of ^{14}C age-offsets in Nikivlik Lake (blue points) and in the LOP section (gold points). Points represent median values of calibrated ^{14}C age-offsets, and bars show the 2σ ranges of age-offsets (LOP; $n = 20$ dates, Nikivlik Lake; $n = 3$ dates). Black and red lines are the mean and 95% upper and lower limits of the interpolated age-offset cubic spline model constructed from the bulk ^{14}C dates. Horizontal gray shading is the 95% range of the age-offset observed from the surface sediments of Nikivlik Lake. Blue shading denotes the Younger Dryas chronozone. The three data points to the left are from Nikivlik Lake, the modern lake that still occupies the LOP basin. Orange shading denotes the Medieval Warm Period chronozone. Gray arrows are periods of lake-level deepening (up) and lowering (down) as inferred by sedimentology.

analogue in Nikivlik Lake, but coarser clastic material and organic-poor sediment suggest that lake-level was lower than during the deposition of Unit 2, or there was an influx of aeolian sand to the lake potentially from nearby point bars in the Etivluk River floodplain.

5.3.1.4. Unit 4: Undisturbed, Deep Water, Organic-Rich Lake Deposit, 11.9–10.2 ka (Lythotypes e and f in Figure 4)

Around 11.9 ka, a single laminated, leaf-debris layer like those found at intermediate depths in Nikivlik Lake today marks the transition to a more organic-rich unit (12.3% mean LOI$_{550°}$). The beginning of this unit marks a major transition where the sediment shifted to relatively low C:N values (11.4 mean) and δ^{13}C values (−29.3‰ mean). Above the leaf-debris layer, this unit is analogous to the deep water Nikivlik Lake deposits that are unaffected by wave base today (Figures 4 and 5).

5.3.1.5. Unit 5: Undisturbed, Shallower, Organic-Rich Lake Deposit With Laminations, 10.2–9.1 ka (Lythotypes e and f in Figure 4)

Laminae composed of repeating layers of sand, silt, and leaves were common in Unit 5 and probably represent storm/poststorm settling events in the lake. This unit was deposited between 10.2 and 9.1 ka. C:N (13.0 mean) and δ^{13}C (−28.4‰ mean) values increased relative to the underlying unit, while organic matter remains relatively high (12.1% mean LOI$_{550°}$). The depositional analogue to this unit is found in the fining-upward, laminated leaf-debris layers that occur in Nikivlik Lake today where wave base occasionally affects the sediment (Figures 4 and 5).

5.3.1.6. Unit 6: Undisturbed, Deep Water, Organic-Poor Lake Deposit, 9.1–5.6 ka (Lythotype e in Figure 4)

The uppermost storm and poststorm settling leaf-debris layers occurred at levels dated to between 9.2 and 8.9 ka where the sediment changed to silt with low organic content (10.7% mean LOI$_{550°}$), while C:N and δ^{13}C values remained similar to those in Unit 5 (Figures 4 and 5). This unit extended upward to the uppermost lake sediment deposited before the lake partly drained shortly after 5.6 ka [*Mann et al.*, 2002]. This unit is analogous to the deep water Nikivlik Lake deposits unaffected by wave base.

5.3.2. LOP and Nikivlik Lake Age-Offsets

In LOP, sediment deposited prior to 14.4 ka had age-offsets ranging from 8.0 to 6.0 ka (not shown). Between 14.4 and 12.8 ka, bulk sediment dates were 5.0 to 6.0 ka older than twigs from the same levels (Figure 6).
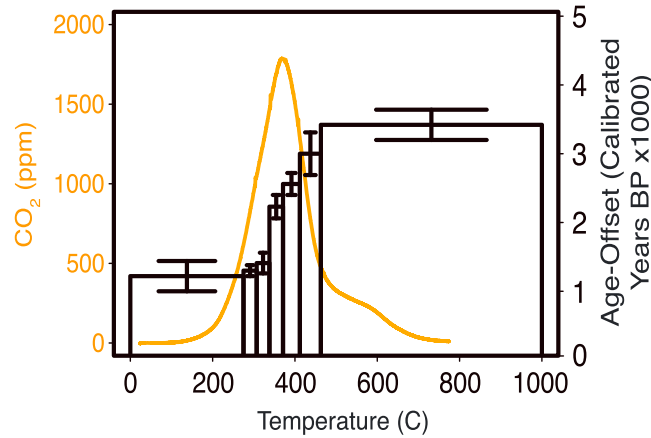
Figure 7. An example of thermogram and ^{14}C age-offsets of ramped-temperature ^{14}C analysis. Data are from Unit 4 in the LOP section. The CO_2 curve is the gas concentrations evolved at successively higher temperatures, and the age-offset shows the ^{14}C age-offset of the gas collected at each temperature step. The age-offset axis is zeroed to the true age for this sediment layer (11.1 ka).

Beginning 12.8 ka, age-offsets declined dramatically to between 2.4 and 1.5 ka until 11.8 ka. Age-offsets between 11.8 and 7.7 ka remained relatively high, ranging from 4.5 to 3.0 ka.

Age-offsets in the 1.7 m water depth core from Nikivlik Lake varied widely over the last four millennia (Figure 6). The age-offsets at 0.13 and 0.26 m depth below the sediment-water interface were 3.3 ka in the horizon with the true age of 3.3 ka, and 5.9 ka in the horizon with the true age of 1.0 ka. Organic matter content (8.8% mean $LOI_{550°}$; not shown) and C:N values (13.3 mean; not shown) did not change between these two horizons; however, particle size did change. This 0.3 m long core was composed of fine sandy silt with the exception of one unit between 0.05 and 0.15 m that was composed of medium to coarse sandy silt with occasional granules. The anomalous age-offset of 5.9 ka that occurs in the horizon with a true age of 1.0 ka was associated with the coarser unit. Neither the Russian nor Bolivia corers could penetrate deeper than 0.3 m into the Nikivlik Lake sediments using human power alone. We suspect that the limited penetration is the result of fine-grained highly compacted sediments in Nikivlik Lake resisting the corer and resulted in an age gap in the LOP and Nikivlik Lake record spanning between 7.7 and 3.3 ka. There is no geomorphic evidence that the lake dried out during this time and caused a sedimentary hiatus.
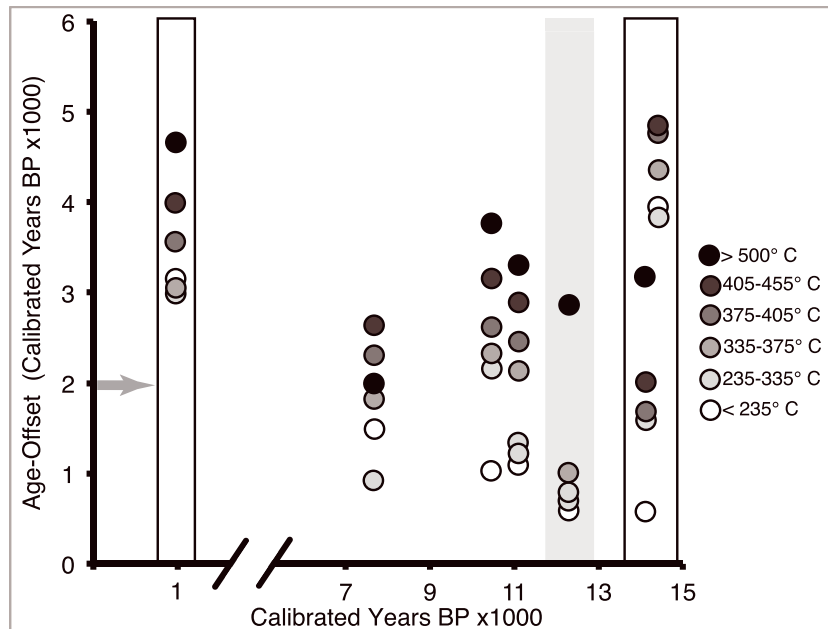

Figure 8. Ramped-temperature ^{14}C age-offsets of individual gas samples and the average temperature range the gas samples were heated. Episodes of inferred thermokarst-driven mass movements are represented by black boxes. Black box on the right is the Bølling-Allerød chronozone while the left black box corresponds to the Medieval Warm Period chronozone. The Younger Dryas chronozone represented in gray shading. Gray arrow is the current age-offset for Nikivlik Lake.
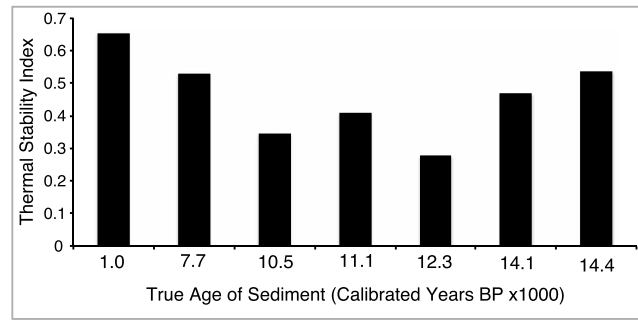
Figure 9. Thermal stability index (TI) calculated from different sediment horizons in the LOP section. Higher indexes indicate sediment that is composed of more recalcitrant organic matter that is more thermally stable.

5.4. Ramped-Temperature [14]C

CO_2 released at different stages in the heating process produced varying ^{14}C ages and age-offsets (i.e., Figures 7 and 8) despite coming from the same sediment sample. Interpolated terrestrial macrofossil ages and median age-offsets of these samples include 14.4 ka (5.3 ka age-offset), 14.1 ka (5.4 ka age-offset), 12.3 ka (1.6 ka age-offset), 11.1 (3.0 ka age-offset; Figure 7), 10.4 (3.0 ka age-offset), and 7.7 (3.5 ka age-offset). Individual age-offsets also varied in the ramped-temperature samples from Nikivlik Lake dated to 1.5 ka (bulk age-offset not measured). Four out of the seven bulk sediment samples used in the ramped-temperature analysis yielded datable gas from all heating fractions. A single gas sample from the 12.3 ka sediment horizon was lost during transfer, and a gas sample from each of the 7.7 ka and 14.4 ka sediment horizons were likely contaminated by modern CO_2 during gas transfer.

The thermal stability index was relatively high in sediment with true calibrated ages of 14.4, 14.1, and 7.7 ka (Figure 9). The highest thermal stability index occurred in the 1.5 ka horizon in Nikivlik Lake. The lowest thermal stability index occurred at the level in LOP with a true age of 12.3 ka. Samples from the 10.4 and 11.1 ka horizons also had relatively low thermal stability indexes. The normalized ages of gas samples were positively correlated with increasing combustion temperature using a general additive model ($R^2 = 0.88$, p value = <0.001; Figure 10). There were two inflection points in the model, one at 300°C and another at around 550°C. The normalized ages of the gas products heated at temperatures <300°C were not significantly different. Above 550°C, the positive relationship between temperature and normalized age again weakened. The sediment layers with reliable ages for all temperature fractions had standard deviations ranging from 540 ^{14}C years from the horizon with the true age of 1.5 ka to 840 ^{14}C years for the horizon with the true age of 10.4 ka (Figure 8). The 14.4 and 11.1 ka samples had standard deviations of 710 and 600 ^{14}C years, respectively.
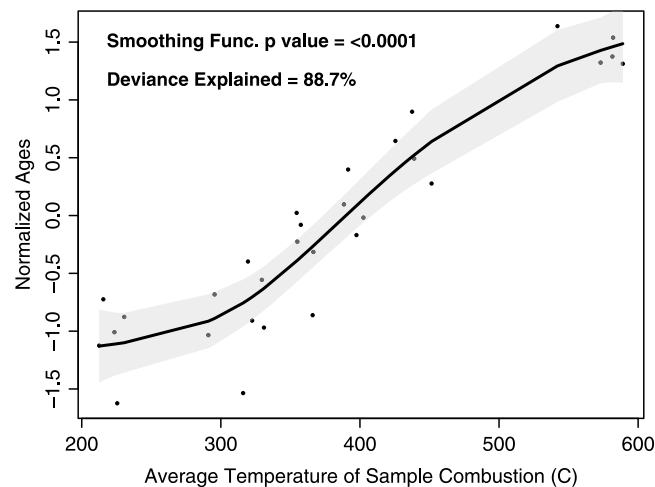

Figure 10. Normalized ^{14}C ages of ramped-temperature gas samples. Black line and gray shading are the mean and 95% confidence intervals for a general additive model fitted to the data. OC that is more resistant to decay has the highest ^{14}C age and is evolved from the sediment sample at the highest temperatures.

5.5. Rates of Total and Ancient OC Deposition in LOP and Nikivlik Lake

Distinct changes occurred in the rates of total OC and ancient OC, defined as the fraction of OC that was >1 ka being deposited in LOP over the last 14.4 ka (Figure 11). Between 14.4 and 13.3 ka, a mean of 14.9 g ancient OC/m²/yr was deposited. Between 13.3 and 11.7 ka, a mean of 5.6 g ancient OC/m²/yr was deposited, and between 11.7 and 10.5 ka, a mean of 8.2 g ancient OC/m²/yr was deposited. Starting at around 10.5 ka, the deposition rates of total OC and ancient OC increased rapidly, with a mean of 21.6 g ancient OC/m²/yr that accumulated until 7.5 ka. In Nikivlik Lake over the past 3.3 ka, a mean of 2.6 g ancient OC/m²/yr was deposited. In total, LOP accumulated 109.7 kg
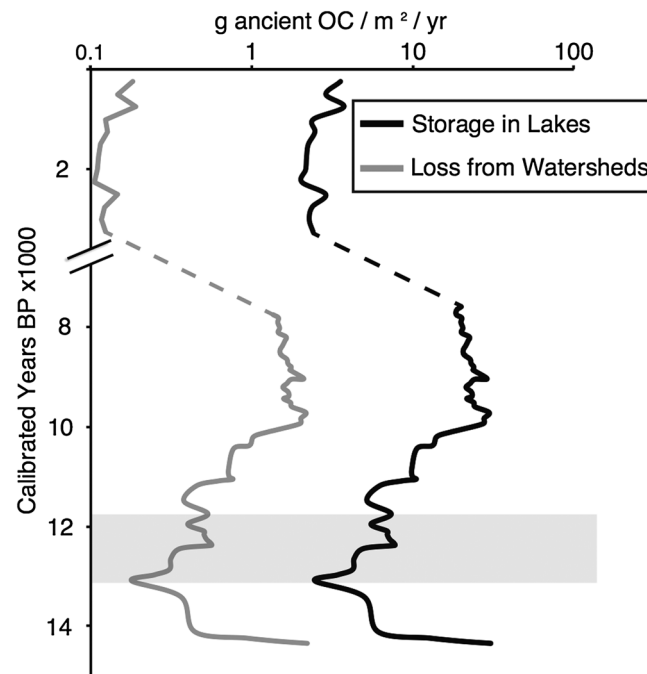
Figure 11. Estimated rates of ancient OC (>1.0 ka OC) deposited in LOP (14.4–7.7 ka) and Nikivlik Lake (3.3 ka–present) on a per year basis (black line). Estimated rates of the loss of ancient OC from the lakes' watersheds (gray line). The dashed line represents the interpolated pattern that occurs during the gap between the LOP and Nikivlik Lake records. Gray shading represents the Younger Dryas chronozone.

total OC/m^2 between 14.4 and 7.7 ka, and 89.6 kg ancient OC/m^2, and 81% of the total OC deposited in LOP was ancient. Nikivlik Lake accumulated 8.5 kg ancient OC/m^2 during the last 3.3 ka. LOP deposited over 6 times as much ancient OC per square meter per millennium as Nikivlik Lake, although this comparison was made using data from different time periods.

6. Discussion

6.1. Interpretation of the Age-Offset Record

Changes in the LOP interpolated age-offset record correspond with climate events during and after the Northern Hemisphere deglaciation (Figures 6 and 12) [*Andersen et al.*, 2004]. Greater-than-present age-offsets and rates of ancient OC deposition in the lake between 14.4 and 12.8 ka and again between 11.9 and 7.7 ka corresponded to periods when climate was warmer than present during the Bølling-Allerød interstadial (14.5–12.9 ka) [*Friedrich et al.*, 2001; *Andersen et al.*, 2004] and the Holocene Thermal Maximum (11.7–9.0 ka) [*Andersen et al.*, 2004; *Kaufman et al.*, 2004]. In the Arctic Foothills, both the Bølling-Allerød and Holocene Thermal Maximum warming events triggered widespread thermokarst-driven mass movements, enhanced erosion, and deeper active layers [*Mann et al.*, 2010]. This geomorphic instability likely involved widespread thermokarst formation in the LOP watershed as well, which would have exhumed aged OC and made it available for downstream transport and redeposition in LOP. Moreover, these warmer-than-present time periods also brought increased effective moisture [*Mann et al.*, 2002], which probably mobilized more aged OC stored in the expanding active layers through leaching and erosion. Lower age-offsets and the lowest ancient OC depositional rates in the record occurred between 12.8 and 11.9 ka during the Younger Dryas chronozone (12.9–11.7 ka), a climate reversion to near-glacial conditions that occurred in many parts of the Northern Hemisphere [*Alley*, 2000; *Andersen et al.*, 2004]. In the Arctic Foothills, the Younger Dryas was accompanied by hillslope stabilization and floodplain incision [*Mann et al.*, 2010], as well as tree line retreat [*Hopkins et al.*, 1981; *Mann et al.*, 2010], and the last occurrence of ice age vegetation in the region [*Mann et al.*, 2002] all of which are indicators of cooler-than-present summer temperatures that probably stabilized permafrost and reduced the deposition of aged OC in LOP.

Two climate- and landscape-mediated mechanisms probably contributed to a decrease in age-offsets and specifically in the deposition rate of ancient (>1 ka) OC between 7.7 ka (the uppermost sample in the LOP section; age-offset 3.5 ka) and today (age-offset 2.0 ka), notwithstanding the record gap between 7.7 and 3.5 ka. First, summer insolation and mean summer temperatures have gradually declined in the Northern Hemisphere over the last 6 ka [*Miller et al.*, 2010]. Second, soil surface organic horizons have progressively spread and accumulated in the Arctic Foothills over the course of the Holocene [*Mann et al.*, 2002; *Jones and Yu*, 2010]. These organic layers on the ground surface insulate the underlying permafrost [*Bockheim et al.*, 1996; *Baughman*, 2013], limiting summer thaw of the active layer. As these soil organic horizons spread, they would have combined with decreasing temperatures during the neoglacial to cool permafrost, reduce active layer thickness, and limit thermal erosion, and so restricted the release of aged OC from permafrost soils.
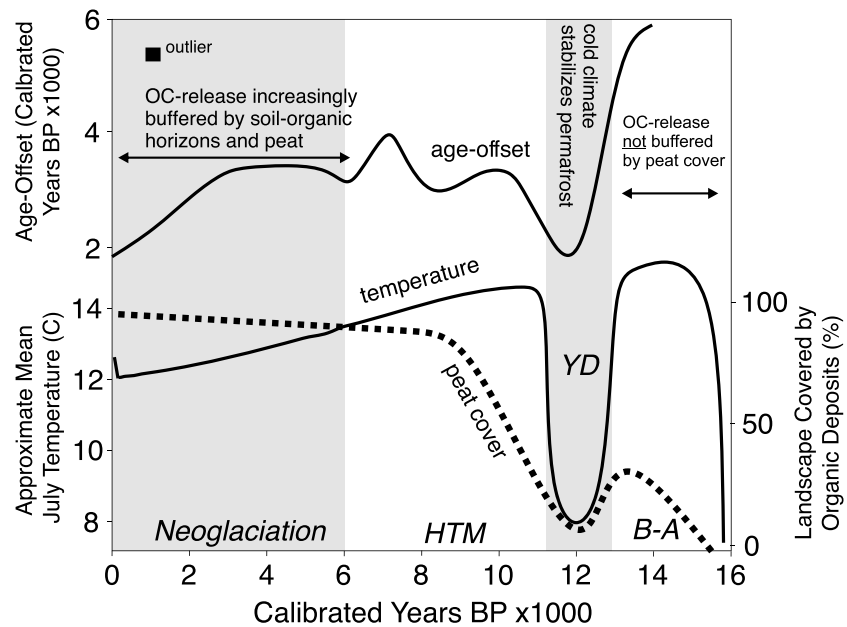
Figure 12. Conceptual model of permafrost OC release over the last 14.5 ka. Approximate mean July temperature curve is from *Mann et al.* [2002, 2010], based on the dates of extralimital *Populus balsamifera* macrofossils as well the magnitude of the Younger Dryas cooling based on *Kokorowski et al.* [2008]. Landscape covered by organic deposits is based on the probability density of basal peat ages from the North Slope of Alaska [*Jones and Yu*, 2010]. Note that the age-offset curve between 7.7 and 3.5 ka is interpolated and actually represents no data because of the age gap between the LOP and Nikivlik Lake record.

There is an anomalous age-offset of 5.9 ka at the horizon with a true age of 1.0 ka in Nikivlik Lake record that we suspect relates to two mass movement scars present on the slope bordering the southwest side of Nikivlik Lake (Figure 1). The flow paths of what were probably two retrogressive-thaw slumps terminate directly in Nikivlik Lake. Mass movements are known to liberate aged organic matter and coarse clastic material into floodplains and lakes [*Frey and McClelland*, 2009; *Lamoureux and Lafrenière*, 2009; *Mesquita et al.*, 2010]. These mass movements were probably responsible for an influx of coarse sand and granules into Nikivlik Lake approximately 1 ka, as well as the unusually high age-offset at this level. Whether or not these thermokarst features were climatically triggered by warming during the Medieval Warm Period [*Miller et al.*, 2010] or represent stochastic geomorphic events is presently unknown.

6.2. Implications for Bulk Sediment [14]C Ages in Paleolimnology Studies

Our results show that ^{14}C ages of bulk lake sediment overestimate the age of a stratigraphic layer and therefore the climate/environmental proxies archived in those layers by thousands of years. Additionally, the magnitude of this overestimate appears to be erratic over time and subject to site-specific variation. Therefore, any paleoenvironmental record whose chronology is based on bulk ^{14}C dates from arctic lakes is clearly suspect.

6.3. Sources of Aged OC

Several lines of evidence suggest autochthonous OC fixed within the lake contributed to the bulk sediment but did not cause the age-offset effect for LOP. First, aquatic macrophytes taking up DIC in the study lakes today have modern ^{14}C signatures (supporting information Table S1). Second, POC entering Nikivlik Lake today is significantly older than the POC leaving the lake or being deposited on the lake bottom. This suggests that autochthonous contributions from phytoplankton and/or macrophytes are "freshening" the sediment with modern OC or that the fresh material is finer and routed through the lake system without being deposited into the sediment [*Goñi et al.*, 1997]. Third, an age-offset from an aquatic macrophyte fragment sampled from LOP was 0.6 ka, which is only a fraction of the bulk sediment median age-offset (2.3 ka) from the same layer. Finally, low-temperature OC fractions, derived from algal material in the Antarctic marine system [*Rosenheim et al.*, 2008], and fresh biogenic OC in the Himalayan rivers [*Rosenheim and Galy*, 2012], had relatively

young ^{14}C ages in every sediment horizon analyzed with ramped-temperature ^{14}C techniques (Figure 10). This pattern implies that algal material deposited in LOP was consistently using near-modern DIC sources and did not contribute a significant aged OC signature to the bulk sediment age.

Changes in lake level could conceivably affect age-offsets by reworking aged OC from either sediment previously deposited on the lake bottom (wave base descends deep as lake-level drops) or by eroding older organic soils through thermokarst processes along the shoreline (lake level rises). Several lines of evidence argue that this process was insignificant in the LOP/Nikivlik records. First, high stands of the lake do not always correspond to shifts in the age-offset record (Figure 6). Second, the numerous ages of twigs and leaves deposited above Unit 1 show no age reversals, which would likely have occurred if some macrofossils had been reworked from older deposits either along the shoreline or on the lake bottom. Similarly, the pollen zonation described from the LOP section by *Mann et al.* [2002] echoes the regional vegetation record, which would not be the case if changes in water level were eroding older, pollen-bearing sediment. A fourth line of evidence comes from the absence in the LOP section above Unit 1 of any sediment types indicative of thermokarst caused by rising lake level [*Hopkins*, 1988; *Murton*, 1996]. Finally, the lithofacies of the nearshore depositional zone in Nikivlik Lake that was frequently disturbed by wave base has no analogue in the LOP section above Unit 1. This indicates the age-offset record we have compiled comes from relatively deep water in a depositional environment where the wave base never dropped low enough to resuspend ancient sediment deposits from the lake bottom. Therefore, the water tracks and streams flowing into LOP/Nikivlik delivered the aged, allochthonous OC causing the observed age-offsets and overshadowed any potential inputs of aged OC from resuspension of older lake sediment or from shoreline erosion of older organic deposits. These multiple lines of evidence strongly suggest that the age-offset record is a proxy for OC release from the LOP/Nikivlik watershed.

The pool of ancient OC released from thawing permafrost that has the greatest potential to provide a positive climate feedback is yedoma, accumulated during the ice ages [*Schirrmeister et al.*, 2012]. The LOP record suggests that yedoma-aged OC in LOP was released only during the Bølling-Allerød warm period, and since then the permafrost containing this very old OC has remained frozen at least at the watershed scale. Supporting evidence is that ramped-temperature gas samples dating to the full glacial (20–16 ka), a period when yedoma accumulation was the dominant process of OC storage in the Arctic Foothills [*Kanevskiy et al.*, 2011], occurred in the 14.4 and 14.1 ka levels in the LOP section. Yedoma OC would have been prone to thaw-triggered mass movements during the Bølling-Allerød because these ice-rich deposits [*Kanevskiy et al.*, 2011] were close to the surface and not yet insulated by soil organic layers [*Jones and Yu*, 2010]. The presence of uninsulated and relatively exposed ancient ice-rich permafrost OC deposits may have primed the Bølling-Allerød period to have produced the oldest OC reworked to LOP/Nikivlik.

6.4. Controls on the Amount and Nature of OC Reworked Into LOP

The nature of the vegetation and soils that initially fixed and stored the aged OC in the LOP watershed determined the amount and quality of OC that eventually transferred into LOP from permafrost and soils. For example, most of the aged OC entering LOP during the Bølling-Allerød period was fixed by terrestrial plants and stored in soils of the mammoth steppe ecosystem [*Guthrie*, 2001]. These ice age soils were relatively poor in OC [*Kanevskiy et al.*, 2011] compared to Holocene soils, generally drier than soils on this landscape today, probably warmer in summer and possibly richer in nutrients [*Hopkins et al.*, 1982; *Walker et al.*, 2001]. These conditions would have been conducive to extensive decomposition of OC and thus left only a recalcitrant fraction to be stored and eventually reworked during the Bølling-Allerød as indicated by the relatively recalcitrant thermal stability index for the sediment laid down in LOP during this time (Figure 9).

The Younger Dryas chronozone had the lowest rates of ancient OC burial, the lowest age-offsets, and the most labile thermal stability index in the LOP record (Figures 6, 8, 9, and 11). These characteristics suggest a reduced input of aged, recalcitrant OC that probably resulted from less permafrost thaw and thinner active layers during the cooler Younger Dryas. Moreover, drier conditions likely occurred during the Younger Dryas as indicated by the presence of xeric tundra pollen types [*Mann et al.*, 2002]. Drier summers would have reduced OC leaching and erosion from the active layer and limited age-offsets. Despite this temporary slowdown of aged OC input to the lake, ancient OC deposition rates were still ~40% of the total OC; thus, even in a cold, dry period similar to the full glacial period in terms of geomorphology and vegetation [*Mann*

et al., 2002], it appears that substantial amounts of ancient OC were still being released from the watershed to subsidize aquatic ecosystems and deposited within the lake.

The highest rates of ancient OC deposition in the LOP/Nikivlik record occurred during the Holocene Thermal Maximum, probably because warming-triggered thaw released aged OC that had accumulated in the carbon-rich soils that developed during the preceding Bølling-Allerød period. Most of the ramped-temperature ^{14}C gas samples from Holocene Thermal Maximum levels in LOP date to the Bølling-Allerød period and therefore come from OC fixed and stored then (Figure 8). Previous studies of peat initiation dates indicate that organic matter accumulated rapidly during this relatively warm, moist time [Mann et al., 2002, 2010; Jones and Yu, 2010], making it a rich source of ancient OC for deposition in LOP in response to early Holocene warming. Lower thermal stability indexes during the Holocene Thermal Maximum levels of LOP may also reflect lower decomposition rates of OC in the increasingly wet and anoxic soils of Bølling-Allerød times (Figure 9). Alternatively, additional allochthonous organic matter inputs to the lake at this time could have fertilized within-lake productivity that may have caused lower thermal stability indexes and lower age-offsets of low-temperature gas samples (Figures 8 and 9). This explanation, which is not mutually exclusive of the abundant-OC one, is supported by a reduction in C:N and δ^{13}C values throughout the Holocene portion of the record (Figure 5).

From the onset of the Holocene up to today, the age of external OC inputs to LOP from its watershed appear to have been increasingly dictated by the buildup of soil surface organic layers and peats. Organic matter accumulating on the ground surface affects the stability of the underlying permafrost by insulating it from surface warming and physically protecting it from thermal and mechanical erosion by running water [McNamara et al., 1998; Shur and Jorgenson, 2007; Baughman, 2013]. These buffering effects of surface soil organic layers and peats first appear in the early Holocene. Thus, even though the Holocene Thermal Maximum experienced warming that was similar to the Bølling-Allerød [Andersen et al., 2004], the resultant age-offsets were much smaller (Figure 6). We suggest the reason for smaller age-offsets is that peat development across the Arctic Foothills insulated the permafrost from the warming climate, which reduced the age and/or the amount of aged OC released. Later, between 10.4 ka and today, OC sources to LOP/Nikivlik became increasingly recalcitrant, declined in age, and had a lower depositional rate of ancient OC. This is what would be expected as accumulating soil surface organic layers and peats progressively sealed off the underlying permafrost sources of OC.

6.5. Quantifying the Ancient OC Lost From Permafrost and Soils

On a global scale, the transfer of SOC from arctic watersheds to depositional environments is a poorly constrained component of OC budgets and may increase during future warming [Mcguire et al., 2009]. What percentage of the OC fixed on the ancient landscape and stored long-term was eventually released and stored in LOP and how do those release rates compare to today? Net ecosystem productivity, the difference between carbon uptake through primary productivity and carbon loss through respiration/lateral transfer, for tussock tundra on the North Slope is an indicator of the how much OC gets stored in soils per year. Long-term estimates of OC storage are appropriate for constraining how much of this SOC is permafrost-bound because of the potential for ongoing OC losses through decomposition in the soil [Trumbore and Harden, 1997; Trumbore, 2000], lateral transfers to freshwaters [Kling et al., 1991], and loss to the atmosphere via wildland fires [Mack et al., 2012; Jones et al., 2013] that occur within years to centuries while OC is stored in the active layer. On millennial timescales, Schell [1983] estimated that ~13 g OC/m^2/yr is stored in tussock tundra on the North Slope. Based on this estimate and scaling the watershed to lake area for Nikivlik Lake, only around 1.4% of this permafrost-bound OC flux estimate is lost from the watershed and redeposited into Nikivlik Lake today on an annual basis. We estimate that during past warming events (i.e., Bølling-Allerød and Holocene Thermal Maximum) ~16% of this permafrost-bound OC was reworked and deposited in LOP based on its watershed to lake area ratio. In other words, 10 times more permafrost-bound SOC was reworked into LOP during warmer-than-present intervals in the past than the permafrost-bound SOC being reworked today.

6.6. Future Warming and Permafrost OC: Lessons From the Past

Despite the rapid warming occurring today in Arctic Alaska, neither the age of the OC being deposited in Nikivlik Lake or the rate of permafrost-bound, ancient OC being deposited are exceptionally elevated today compared to those observed over the last 14.4 ka (Figures 6, 8, 11, and 12). In fact, the age-offsets

and depositional rates observed today are similar to those that occurred during the Younger Dryas when summer temperatures were at least 2°C cooler than present [*Kokorowski et al.*, 2008; *Mann et al.*, 2010]. This observation strongly suggests that recent warming in the Arctic Foothills has not yet enhanced OC release from the active layers and permafrost in the LOP watershed.

Our time series of age-offsets suggests that the threshold temperature at which warming will trigger widespread OC release from permafrost watersheds has risen significantly over the course of deglacial times up to the present. This threshold has probably risen because of the progressive spread and accumulation of surface soil organic layers and peats across the Arctic Foothills during postglacial times. For the future warming to trigger enhanced OC release through permafrost thaw, it must exceed the insulating capacity of this organic mat. Alternatively, these surface layers would have to be removed by disturbances like tundra fires and mass movements. Only after the thermal buffering effect of the organic mat is removed or surpassed by warming will widespread thaw of permafrost occur and abundant Holocene-aged OC be released into aquatic ecosystems and potentially the atmosphere.

7. Conclusions

Age-offsets between a sediment layer's true age of deposition (determined by ^{14}C dating delicate, terrestrial plant macrofossils) and the apparent age of the same sediment layer (determined by dating the sediment matrix enclosing each macrofossil) can be used to gauge how the OC stored on a permafrost landscape responded to climate change in the past. Today, age-offsets in a typical permafrost watershed in Arctic Alaska are ~2.0 ka, which is indicative of slow-cycling OC pools whose dynamics are controlled by decay-resistant vegetation, shallow active layers, and underlying permafrost. Earlier in postglacial times when summer air temperatures were ~2–3°C warmer than today, age-offsets were 3–5 ka. During these previous relatively warm periods, the Bølling-Allerød interstadial (14.5–12.9 ka) and the Holocene Thermal Maximum (11.7–8.0 ka), rates of ancient OC release from the watershed were up to 10 times greater than those of today. In contrast, during the relatively cold Younger Dryas (12.9–11.7 ka), age-offsets and both total and ancient OC transfers from the watershed to the lake were similar to those of today. The erratic behavior of age-offsets and the overestimate of bulk sediment ages discredit the chronologies of paleoclimate studies based on bulk lake sediment ages. Contemporary age-offsets similar to the colder-than-present Younger Dryas is probably the result of the peat and surface soil organic layers that have progressively spread and accumulated in the Arctic Foothills beginning in the early Holocene. The insulating effects of this organic cover has probably limited permafrost thaw over the course of the Holocene. Exceptions to this trend occur when isolated mass movements disrupt the insulative cover, trigger the thaw of permafrost containing organic matter, and so generate pulses of ancient OC into the lake, as we think occurred approximately 1.0 ka in Nikivlik Lake. The temperature-buffering effects of surface organic layers have likely raised the air temperature threshold above which widespread thawing of permafrost can occur in the Arctic Foothills. This threshold may be higher than it has been at any time in the past 14.4 ka. Although climate is warming rapidly in the Arctic, this warming has yet to enhance the mobilization of vast stores of ancient OC stored in active layers and permafrost in the Arctic Foothills of Alaska.

References

Abbott, M. B., and T. W. Stafford Jr. (1996), Radiocarbon geochemistry of modern and ancient arctic lake systems, Baffin Island, Canada, *Quat. Res.*, 45(3), 300–311, doi:10.1006/qres.1996.0031.

Algesten, G., S. Sobek, A. K. Bergström, A. Jonsson, L. J. Tranvik, and M. Jansson (2005), Contribution of sediment respiration to summer CO_2 emission from low productive boreal and subarctic lakes, *Microb. Ecol.*, 50(4), 529–535, doi:10.1007/s00248-005-5007-x.

Alley, R. B. (2000), The Younger Dryas cold interval as viewed from central Greenland, *Quat. Sci. Rev.*, 19(1), 213–226, doi:10.1016/S0277-3791(99)00062-1.

Anchukaitis, K. J., R. D. D'Arrigo, L. Andreu-Hayles, D. Frank, A. Verstege, A. Curtis, B. M. Buckley, G. C. Jacoby, and E. R. Cook (2013), Tree-ring-reconstructed summer temperatures from Northwestern North America during the last nine centuries, *J. Clim.*, 26(10), 3001–3012, doi:10.1175/JCLI-D-11-00139.1.

Andersen, K. K., et al. (2004), High-resolution record of Northern Hemisphere climate extending into the last interglacial period, *Nature*, 431(7005), 147–151, doi:10.1038/nature02805.

Anderson, L., M. B. Abbott, and B. P. Finney (2001), Holocene climate inferred from oxygen isotope ratios in lake sediments, Central Brooks Range, Alaska, *Quat. Res.*, 55(3), 313–321, doi:10.1006/qres.2001.2219.

Badding, M. E., J. P. Briner, and D. S. Kaufman (2012), ^{10}Be ages of late Pleistocene deglaciation and Neoglaciation in the north-central Brooks Range, Arctic Alaska, *J. Quat. Sci.*, 28(1), 95–102, doi:10.1002/jqs.2596.

Baffi, C., M. T. Dell'Abate, A. Nassisi, S. Silva, A. Benedetti, P. L. Genevini, and F. Adani (2007), Determination of biological stability in compost: A comparison of methodologies, *Soil Biol. Biochem.*, 39(6), 1284–1293, doi:10.1016/j.soilbio.2006.12.004.

Baughman, C. A. (2013), Soil surface organic layers in the Arctic Foothills: Distribution, development and microclimate feedbacks, MS thesis, Department of Geography, University of Alaska Fairbanks, Fairbanks.

Billings, W. D. (1987), Carbon balance of Alaskan tundra and taiga ecosystems: Past, present and future, *Quat. Sci. Rev.*, *6*(2), 165–177, doi:10.1016/0277-3791(87)90032-1.

Bird, B. W., M. B. Abbott, B. P. Finney, and B. Kutchko (2008), A 2000 year varve-based climate record from the central Brooks Range, Alaska, *J. Paleolimnol.*, *41*(1), 25–41, doi:10.1007/s10933-008-9262-y.

Blaauw, M. (2010), Methods and code for "classical" age-modeling of radiocarbon sequences, *Quat. Geochronol.*, *5*(5), 512–518, doi:10.1016/j.quageo.2010.01.002.

Bockheim, J. G. (2007), Importance of cryoturbation in redistributing organic carbon in permafrost-affected soils, *Soil Sci. Soc. Am. J.*, *71*(4), 1335–1342, doi:10.2136/sssaj2006.0414N.

Bockheim, J. G., D. A. Walker, and L. R. Everett (1996), Soil carbon distribution in nonacididc and acidic tundra of Arctic Alaska, in *Soil Processes and the Carbon Cycle*, edited by R. Lal et al., pp. 143–155, CRC Press, New York.

Brock, F., T. Higham, P. Ditchfield, and C. B. Ramsey (2010), Current pretreatment methods for AMS radiocarbon dating at the Oxford Radiocarbon Accelerator Unit (ORAU), *Radiocarbon*, *52*(1), 103–112.

Calkin, P. E. (1988), Holocene glaciation of Alaska (and adjoining Yukon Territory, Canada), *Quat. Sci. Rev.*, *7*(2), 159–184, doi:10.1016/0277-3791(88)90004-2.

Carper, G. L., and R. W. Bachmann (1984), Wind resuspension of sediments in a prairie lake, *Can. J. Fish.*, *41*(12), 1763–1767, doi:10.1139/f84-217.

Edwards, K. J., and G. Whittington (2001), Lake sediments, erosion and landscape change during the Holocene in Britain and Ireland, *Catena*, *42*(2–4), 143–173, doi:10.1016/S0341-8162(00)00136-3.

French, H. (2010), *The Periglacial Environment*, John Wiley, New York.

Frey, K. E., and J. W. McClelland (2009), Impacts of permafrost degradation on arctic river biogeochemistry, *Hydrol. Processes*, *23*(1), 169–182, doi:10.1002/hyp.7196.

Friedrich, M., B. Kromer, K. F. Kaiser, and M. Spurk (2001), High-resolution climate signals in the Bølling–Allerød Interstadial (Greenland Interstadial 1) as reflected in European tree-ring chronologies compared to marine varves and ice-core records, *Quat. Sci. Rev.*, *20*(11), 1223–1232, doi:10.1016/S0277-3791(00)00148-7.

Geirsdóttir, Á., G. H. Miller, T. Thordarson, and K. B. Ólafsdóttir (2009), A 2000 year record of climate variations reconstructed from Haukadalsvatn, West Iceland, *J. Paleolimnol.*, *41*(1), 95–115, doi:10.1007/s10933-008-9253-z.

Goñi, M. A., K. C. Ruttenberg, and T. I. Eglinton (1997), Sources and contribution of terrigenous organic carbon to surface sediments in the Gulf of Mexico, *Nature*, *389*(6648), 275–278, doi:10.1016/s0016-7037(02)01412-6.

Grunblatt, J., and D. Atwood Jr. (2014), Mapping lakes for winter liquid water availability using SAR on the North Slope of Alaska, *Int. J. Appl. Earth Obs. Geoinf.*, *27*, 63–69.

Guo, L., and R. W. Macdonald (2006), Source and transport of terrigenous organic matter in the upper Yukon River: Evidence from isotope (δ^{13}C, Δ^{14}C, and δ^{15}N) composition of dissolved, colloidal, and particulate phases, *Global Biogeochem. Cycles*, *20*, GB2011, doi:10.1029/2005GB002593.

Guo, L., C. L. Ping, and R. W. Macdonald (2007), Mobilization pathways of organic carbon from permafrost to arctic rivers in a changing climate, *Geophys. Res. Lett.*, *34*, L13603, doi:10.1029/2007GL030689.

Gustafsson, Ö., B. E. van Dongen, J. E. Vonk, O. V. Dudarev, and I. P. Semiletov (2011), Widespread release of old carbon across the Siberian Arctic echoed by its large rivers, *Biogeosci. Discuss.*, *8*(1), 1445–1461, doi:10.5194/bgd-8-1445-2011.

Guthrie, R. D. (2001), Origin and causes of the mammoth steppe: A story of cloud cover, woolly mammal tooth pits, buckles, and inside-out Beringia, *Quat. Sci. Rev.*, *20*(1), 549–574, doi:10.1016/S0277-3791(00)00099-8.

Hågvar, S., and M. Ohlson (2013), Ancient carbon from a melting glacier gives high 14C age in living pioneer invertebrates, *Sci. Rep.*, *3*, 2820, doi:10.1038/srep02820.

Håkanson, L. J., and M. Jansson (2002), *Principles of Lake Sedimentology*, Blackburn Press, New York.

Hamilton, T. D. (2001), Quaternary glacial, lacustrine, and fluvial interactions in the western Noatak basin, Northwest Alaska, *Quat. Sci. Rev.*, *20*(1–3), 371–391, doi:10.1016/S0277-3791(00)00110-4.

Heimann, M., and M. Reichstein (2008), Terrestrial ecosystem carbon dynamics and climate feedbacks, *Nature*, *451*(7176), 289–292, doi:10.1038/nature06591.

Heiri, O., A. F. Lotter, and G. Lemcke (2001), Loss on ignition as a method for estimating organic and carbonate content in sediments: Reproducibility and comparability of results, *J. Paleolimnol.*, *25*(1), 101–110, doi:10.1023/A:1008119611481.

Hinzman, L. D., et al. (2005), Evidence and implications of recent climate change in northern Alaska and other Arctic regions, *Clim. Change*, *72*(3), 251–298, doi:10.1007/s10584-005-5352-2.

Hopkins, D. M. (1988), Thaw lake sediments and sedimentary environments, in *Permafrost: Proceedings of the Fifth International Conference on Permafrost*, pp. 790–795, Tapir Publishers, Trondheim.

Hopkins, D. M., P. A. Smith, and J. V. Matthews Jr. (1981), Dated wood from Alaska and the Yukon: Implications for forest refugia in Beringia, *Quat. Res.*, *15*(3), 217–249, doi:10.1016/0033-5894(81)90028-4.

Hopkins, D. M., J. V. Matthews Jr., C. E. Schweger, and S. B. Young (Eds.) (1982), *Paleoecology of Beringia*, Wiley and Sons, New York.

Jones, M. C., and Z. Yu (2010), Rapid deglacial and early Holocene expansion of peatlands in Alaska, *Proc. Natl. Acad. Sci. U.S.A.*, *107*(16), 7347–7352, doi:10.1073/pnas.0911387107.

Jones, B. M., A. Breen, B. V. Gaglioti, D. H. Mann, A. V. Rocha, G. Grosse, C. Arp, M. Kunz, and D. Walker (2013), Identification of unrecognized tundra fire events on the north slope of Alaska, *J. Geophys. Res. Biogeosci.*, *118*, 1334–1344, doi:10.1002/jgrg.20113.

Kanevskiy, M., Y. Shur, D. Fortier, M. T. Jorgenson, and E. Stephani (2011), Cryostratigraphy of late Pleistocene syngenetic permafrost (yedoma) in northern Alaska, Itkillik River exposure, *Quat. Res.*, *75*(3), 584–596, doi:10.1016/j.yqres.2010.12.003.

Kaufman, D. S., et al. (2004), Holocene thermal maximum in the western Arctic (0–180°W), *Quat. Sci. Rev.*, *23*(5–6), 529–560, doi:10.1016/j.quascirev.2003.09.007.

Kaufman, D. S., et al. (2009), Recent warming reverses long-term Arctic cooling, *Science*, *325*(5945), 1236–1239, doi:10.1126/science.1173983.

Kling, G. W., G. W. Kipphut, and M. C. Miller (1991), Arctic lakes and streams as gas conduits to the atmosphere: Implications for tundra carbon budgets, *Science*, *251*(4991), 298–301, doi:10.1126/science.251.4991.298.

Kokorowski, H. D., P. M. Anderson, C. J. Mock, and A. V. Lozhkin (2008), A re-evaluation and spatial analysis of evidence for a Younger Dryas climatic reversal in Beringia, *Quat. Sci. Rev.*, *27*(17–18), 1710–1722, doi:10.1016/j.quascirev.2008.06.010.

Lamoureux, S. F., and M. J. Lafrenière (2009), Fluvial impact of extensive active layer detachments, Cape Bounty, Melville Island, Canada, *Arct. Antarct. Alp. Res.*, *41*(1), 59–68, doi:10.1657/1523-0430-41.1.59.

Lamoureux, S. F., and M. J. Lafrenière (2014), Seasonal fluxes and age of particulate organic carbon exported from Arctic catchments impacted by localized permafrost slope disturbances, *Environ. Res. Lett.*, *9*(4), 045002, doi:10.1088/1748-9326/9/4/045002.

Mack, M. C., M. S. Bret-Harte, T. N. Hollingsworth, R. R. Jandt, E. A. Schuur, G. R. Shaver, and D. L. Verbyla (2012), Carbon loss from an unprecedented Arctic tundra wildfire, *Nature*, *475*(7357), 489–492, doi:10.1038/nature10283.

Mann, D. H., D. M. Peteet, R. E. Reanier, and M. L. Kunz (2002), Responses of an arctic landscape to late glacial and early Holocene climatic changes: The importance of moisture, *Quat. Sci. Rev.*, *21*(8–9), 997–1021, doi:10.1016/S0277-3791(01)00116-0.

Mann, D. H., P. Groves, R. E. Reanier, and M. L. Kunz (2010), Floodplains, permafrost, cottonwood trees, and peat: What happened the last time the climate warmed suddenly in arctic Alaska, *Quat. Sci. Rev.*, *29*(27–28), 3812–3830, doi:10.1016/j.quascirev.2010.09.002.

McGuire, A. D., L. G. Anderson, T. R. Christensen, S. Dallimore, L. Guo, D. J. Hayes, M. Heimann, T. D. Loreenson, R. W. Macdonald, and N. Roulet (2009), Sensitivity of the carbon cycle in the Arctic to climate change, *Ecol. Monogr.*, *79*(4), 523–555, doi:10.1890/08-2025.1.

McNamara, J. P., D. L. Kane, and L. D. Hinzman (1998), An analysis of streamflow hydrology in the Kuparuk River Basin, Arctic Alaska: A nested watershed approach, *J. Hydrol.*, *206*(1), 39–57, doi:10.1016/S0022-1694(98)00083-3.

Mesquita, P. S., F. J. Wrona, and T. D. Prowse (2010), Effects of retrogressive permafrost thaw slumping on sediment chemistry and sub-merged macrophytes in Arctic tundra lakes, *Freshwater Biol.*, *55*(11), 2347–2358, doi:10.1111/j.1365-2427.2010.02450.x.

Meyers, P. A., and R. Ishiwatari (1993), Lacustrine organic geochemistry—An overview of indicators of organic matter sources and diagenesis in lake sediments, *Org. Geochem.*, *20*(7), 867–900, doi:10.1016/0146-6380(93)90100-P.

Miller, G. H., et al. (2010), Temperature and precipitation history of the Arctic, *Quat. Sci. Rev.*, *29*(15–16), 1679–1715, doi:10.1016/j.quascirev.2010.03.001.

Murton, J. B. (1996), Thermokarst-lake-basin sediments, Tuktoyaktuk Coastlands, western arctic Canada, *Sedimentology*, *43*(4), 737–760, doi:10.1111/j.1365-3091.1996.tb02023.x.

Oswald, W. W., L. B. Brubaker, F. S. Hu, and G. W. Kling (2003), Holocene pollen records from the central Arctic Foothills, northern Alaska: Testing the role of substrate in the response of tundra to climate change, *J. Ecol.*, *91*(6), 1034–1048, doi:10.1046/j.1365-2745.2003.00833.x.

Oswald, W. W., P. M. Anderson, T. A. Brown, L. B. Brubaker, H. Feng Sheng, A. V. Lozhkin, W. Tinner, and P. Kaltenrieder (2005), Effects of sample mass and macrofossil type on radiocarbon dating of arctic and boreal lake sediments, *Holocene*, *15*(5), 758–767, doi:10.1191/0959683605hl849rr.

Plante, A. F., J. M. Fernández, and J. Leifeld (2009), Application of thermal analysis techniques in soil science, *Geoderma*, *153*(1–2), 1–10, doi:10.1016/j.geoderma.2009.08.016.

Pons, L., H. Lambers, and F. S. Chapin III (1998), *Plant Physiological Ecology*, Springer, New York.

Raymond, P. A., J. W. McClelland, and R. M. Holmes (2007), Flux and age of dissolved organic carbon exported to the Arctic Ocean: A carbon isotopic study of the five largest arctic rivers, *Global Biogeochem. Cycles*, *21*, GB4011, doi:10.1029/2007GB002934.

Raynolds, M. K., D. A. Walker, and H. A. Maier (2005), Plant community-level mapping of arctic Alaska based on the Circumpolar Arctic Vegetation Map, *Phytocoenologia*, *35*(4), 821–848, doi:10.1127/0340-269X/2005/0035-0821.

Reimer, P. J., et al. (2013), IntCal13 and Marine13 radiocarbon age calibration curves 0–50,000 years cal BP, *Radiocarbon*, *55*(4), 1869–1887, doi:10.2458/azu_js_rc.55.16947.

Reyes, A. V., D. G. Froese, and B. J. Jensen (2010), Permafrost response to last interglacial warming: Field evidence from non-glaciated Yukon and Alaska, *Quat. Sci. Rev.*, *29*(23), 3256–3274, doi:10.1016/j.quascirev.2010.07.013.

Rosenheim, B. E., and V. Galy (2012), Direct measurement of riverine particulate organic carbon age structure, *Geophys. Res. Lett.*, *39*, L19703, doi:10.1029/2012GL052883.

Rosenheim, B. E., M. B. Day, E. Domack, H. Schrum, A. Benthien, and J. M. Hayes (2008), Antarctic sediment chronology by programmed-temperature pyrolysis: Methodology and data treatment, *Geochem. Geophys. Geosyst.*, *9*, Q04005, doi:10.1029/2007GC001816.

Rosenheim, B. E., K. M. Roe, B. J. Roberts, A. S. Kolker, M. A. Allison, and K. H. Johannesson (2013a), River discharge influences on particulate organic carbon age structure in the Mississippi/Atchafalaya River System, *Global Biogeochem. Cycles*, *27*, 154–166, doi:10.1002/gbc.20018.

Rosenheim, B. E., J. A. Santoro, M. Gunter, and E. W. Domack (2013b), Improving Antarctic sediment ^{14}C dating using ramped pyrolysis: An example from the Hugo Island trough, *Radiocarbon*, *55*(1), 115–126, doi:10.2458/azu_js_rc.v55i1.16234.

Schaefer, K., T. Zhang, L. Bruhwiler, and A. P. Barrett (2011), Amount and timing of permafrost carbon release in response to climate warming, *Tellus B*, *63*(2), 165–180, doi:10.1111/j.1600-0889.2011.00527.x.

Schell, D. M. (1983), Carbon-13 and carbon-14 abundances in Alaskan aquatic organisms: Delayed production from peat in arctic food webs, *Science*, *219*(4588), 1068–1071, doi:10.1126/science.219.4588.1068.

Schirrmeister, L., D. Froese, V. Tumskoy, and S. Wetterich (2012), Yedoma: Late Pleistocene ice-rich syngenetic permafrost of Beringia, in *The Encyclopedia of Quaternary Science*, 2nd ed., edited by S. A. Elias, C. J. Mock, and J. Murton, pp. 542–552, Elsevier, Amsterdam, doi:10.1016/b978-0-444-53643-3.00106-0.

Schreiner, K. M., T. S. Bianchi, and B. E. Rosenheim (2014), Evidence for permafrost thaw and transport from an Alaskan North Slope watershed, *Geophys. Res. Lett.*, *41*, 3117–3126, doi:10.1002/2014gl059514.

Schuur, E. A. G., J. Bockheim, J. G. Canadell, and E. Euskirchen (2008), Vulnerability of permafrost carbon to climate change: Implications for the global carbon cycle, *BioScience*, *58*(8), 701–714, doi:10.1641/B580807.

Schuur, E. A. G., J. G. Vogel, K. G. Crummer, H. Lee, J. O. Sickman, and T. E. Osterkamp (2009), The effect of permafrost thaw on old carbon release and net carbon exchange from tundra, *Nature*, *459*(7246), 556–559, doi:10.1038/nature08031.

Shur, Y. L., and M. T. Jorgenson (2007), Patterns of permafrost formation and degradation in relation to climate and ecosystems, *Permafrost Periglac. Processes*, *18*(1), 7–19, doi:10.1002/ppp.582.

Stafford, J. M., G. Wendler, and J. Curtis (2000), Temperature and precipitation of Alaska: 50 year trend analysis, *Theor. Appl. Climatol.*, *67*(1–2), 33–44, doi:10.1007/s007040070014.

Tarnocai, C., J. G. Canadell, E. A. G. Schuur, P. Kuhry, G. Mazhitova, and S. Zimov (2009), Soil organic carbon pools in the northern circumpolar permafrost region, *Global Biogeochem. Cycles*, *23*, GB2023, doi:10.1029/2008GB003327.

Trumbore, S. (2000), Age of soil organic matter and soil respiration: Radiocarbon constraints on belowground C dynamics, *Ecol. Appl.*, *10*(2), 399–411, doi:10.1890/1051-0761.

Trumbore, S. E., and J. W. Harden (1997), Accumulation and turnover of carbon in organic and mineral soils of the BOREAS northern study area, *J. Geophys. Res.*, *102*(D24), 28,817–28,830, doi:10.1029/97JD02231.

Vonk, J. E., and Ö. Gustafsson (2013), Permafrost-carbon complexities, *Nature*, *6*(9), 675–676, doi:10.1038/ngeo1937.

Vonk, J. E., B. E. van Dongen, and Ö. Gustafsson (2010), Selective preservation of old organic carbon fluvially released from sub-Arctic soils, *Geophys. Res. Lett.*, *37*, L11605, doi:10.1029/2010GL042909.

Vonk, J. E., V. Alling, L. Rahm, C.-M. Mörth, C. Humborg, and Ö. Gustafsson (2012), A centennial record of fluvial organic matter input from the discontinuous permafrost catchment of Lake Torneträsk, *J. Geophys. Res.*, *117*, G03018, doi:10.1029/2011JG001887.

Wachenfeldt, E. V., and L. J. Tranvik (2008), Sedimentation in boreal lakes—The role of flocculation of allochthonous dissolved organic matter in the water column, *Ecosystems*, *11*(5), 803–814, doi:10.1007/s10021-008-9162-z.

Walker, D. A., J. G. Bockheim, F. S. Chapin III, W. Eugster, F. E. Nelson, and C. L. Ping (2001), Calcium-rich tundra, wildlife, and the "Mammoth Steppe", *Quat. Sci. Rev.*, *20*(1), 149–163, doi:10.1016/S0277-3791(00)00126-8.

Walker, D. A., et al. (2005), The Circumpolar Arctic Vegetation Map, *J. Veg. Sci.*, *16*(3), 267–282, doi:10.1111/j.1654-1103.2005.tb02365.x.

Walter, K. M., S. A. Zimov, J. P. Chanton, D. Verbyla, and F. S. Chapin (2006), Methane bubbling from Siberian thaw lakes as a positive feedback to climate warming, *Nature*, *443*(7107), 71–75, doi:10.1038/nature05040.

Walter, K. M., M. E. Edwards, G. Grosse, S. A. Zimov, and F. S. Chapin (2007), Thermokarst lakes as a source of atmospheric CH4 during the last deglaciation, *Science*, *318*(5850), 633–636, doi:10.1126/science.1142924.

Wolfe, A. P., G. H. Miller, C. A. Olsen, S. L. Forman, P. T. Doran, and S. U. Holmgren (2004), Geochronology of high latitude lake sediments, in *Long-Term Environmental Change in Arctic and Antarctic Lakes*, pp. 19–52, Springer, Netherlands, doi:10.1007/978-1-4020-2126-8_2.

Wooller, M. J., J. W. Pohlman, B. V. Gaglioti, P. Langdon, M. Jones, K. M. W. Anthony, K. W. Becker, K.-U. Hinrichs, and M. Elvert (2012), Reconstruction of past methane availability in an Arctic Alaska wetland indicates climate influenced methane release during the past ~ 12,000 years, *J. Paleolimnol.*, *48*(1), 27–42, doi:10.1007/s10933-012-9591-8.